Journal of Materials Chemistry A

ROYAL SOCIETY OF CHEMISTRY

REVIEW

View Article Online
View Journal

Cite this: DOI: 10.1039/d5ta00834d

Mixed matrix membranes for hydrogen separation: a comprehensive review and performance analysis†

Reza Sabouri, Bradley Paul Ladewig * and Nicholaus Prasetya *

Hydrogen has emerged as one of the cleanest energy vectors that can support the transition into a green economy and thus can facilitate the transition to a carbon-neutral environment. Common hydrogen production methods include coal gasification, steam reforming, methane pyrolysis, and water electrolysis. All the hydrogen production methods produce a mixture of H_2 and other products such as CO_2, N_2 and CH_4 depending on the method. To separate hydrogen from other molecules, common methods such as cryogenic distillation and pressure swing adsorption have been used widely. In addition to these methods, membranes can be used which offer energy efficiency compared to the previously mentioned methods. The widely used membranes for H_2 separation are metallic membranes such as palladium-based membranes. Despite their high separation performance, they are not cost-effective. Another type of membrane that can address cost-efficiency, energy consumption, and performance limitations is the polymeric membrane. Moreover, polymeric membranes are also solution-processable and thus offer another advantage from a fabrication point of view. However, polymeric membranes usually suffer from a permeability-selectivity trade-off. Therefore, there is a need to improve the hydrogen separation performance of polymeric membranes, and one effective strategy is to form mixed matrix membranes (MMMs). MMMs are composite membranes composed of at least two components: polymers and fillers. The presence of fillers in this type of membrane is important to improve the separation performance of polymeric membranes. This review then aims to provide an overview of MMMs used for hydrogen separation, starting from their fabrication strategies until thorough discussions and assessments of different fillers. Moreover, this article also comprehensively evaluates the performance of MMMs by assessing their improvement in the separation performance and scrutinizing the impact of the filler's physical properties on the MMM performance. Lastly, the outlook of the field is also given to direct future research in this field.

Received 31st January 2025
Accepted 20th May 2025

DOI: 10.1039/d5ta00834d

rsc.li/materials-a

Paul Wurth Chair, Department of Engineering, Faculty of Science, Technology and Medicine, University of Luxembourg, 2, Place de l'Université, L-4365 Esch-sur-Alzette, Luxembourg. E-mail: bradley.ladewig@uni.lu; nicholaus.prasetya@uni.lu

† Electronic supplementary information (ESI) available. See DOI: https://doi.org/10.1039/d5ta00834d

Reza Sabouri

Reza Sabouri is currently a PhD researcher in the Paul Wurth Chair at the University of Luxembourg. He obtained his bachelor's degree from the Sahand University of Technology in 2018 and his master's degree from Istanbul Technical University in 2023. His research focuses on gas separation and hydrogen purification using advanced porous materials such as MOFs and COFs, particularly in the development of high-performance mixed matrix membranes (MMMs) aimed at enabling efficient and sustainable solutions for clean energy and environmental technologies.

Bradley Paul Ladewig

Prof. Bradley Paul Ladewig is currently a Paul Wurth Chair professor of energy engineering and a vice dean in the faculty of engineering, University of Luxembourg. He obtained his PhD degree in 2006 from the University of Queensland, Australia. He has an extensive international academic career starting by joining Monash University (2009–2015), followed by Imperial College London (2015–2018) and the Institute of Micro Process Engineering, Karlsruhe Institute of Technology (KIT) (2018–2022). His research interests are in the field of clean energy and separation processes, particularly advanced membrane technologies.

1. Introduction

With the growing concern about the continuous increase of the global temperature, there is also an urgent need to accelerate the transition process from a fossil fuel-based economy to a green economy. In this respect, introducing hydrogen as one of the cleanest energy carriers is one of the major ways to accelerate the transition process. Within this context, advancing the hydrogen purification process is one of the most crucial aspects in addition to the hydrogen production process. This is because, in most cases, hydrogen will be produced alongside other light gases. For example, when hydrogen is produced by a steam reforming process, it must be separated from carbon dioxide and unreacted methane. In another case, where ammonia cracking is chosen as the method to produce hydrogen, the separation process of hydrogen from nitrogen becomes necessary. Moreover, in the perspective of hydrogen distribution, it might also be essential to utilize well-developed natural gas pipelines. In this case, hydrogen will be mixed with natural gas during the distribution and therefore requires a separation process if the end users demand pure hydrogen for their needs. Different separation technologies are available to carry out this task such as adsorption, cryogenic distillation and membrane separation. Compared with other technologies, membrane separation technology could offer numerous advantages such as high performance, low energy consumption and a low carbon footprint. Therefore, advancing the membrane-based hydrogen separation process could also become one of the key steps in facilitating the adoption of hydrogen for the green economy transition.

Until now, hydrogen separation membranes can be fabricated from different materials such as metals or metal alloys, metal organic frameworks (MOFs), polymers and zeolites. Among these options, polymers could still be considered one of the most promising materials, particularly from the economical and fabrication perspectives because they are relatively cheap and solution-processable.[1] Both advantages also lead to another key positive aspect of polymers, namely their ease of processing to be turned into a commercial membrane module.[2] However, such advantages come with a couple of drawbacks. As was elucidated by Robeson, polymeric membranes suffer from the permeability-selectivity trade-off. Therefore, membranes with high permeability usually exhibit low selectivity and *vice versa*.[3] In addition, polymeric membranes also face another challenge related to their separation performance instability which can be brought on by different factors such as plasticization and physical aging.[2]

Therefore, to effectively address these drawbacks, various strategies have been proposed to significantly improve the gas separation performance of polymeric membranes. One of the main strategies is to fabricate mixed matrix membranes (MMMs). In this case, a discrete phase, which is called the filler, is incorporated into a polymeric matrix acting as the continuous phase. The incorporation of such fillers has then been demonstrated for being able to improve the polymeric membrane performance not only by increasing its gas separation performance but also by reducing the plasticization and physical aging effects. This review article then aims to comprehensively discuss the recent advances in the field of MMMs used particularly for hydrogen separation. Various fillers that have been investigated will be extensively discussed and the performance of the resulting MMMs will also be comprehensively analyzed. It is anticipated that such an analysis could bring a new insight regarding the current performance of MMMs for hydrogen separation and thus provide a direction for future research.

Nicholaus Prasetya

Dr Nicholaus Prasetya is currently a research associate in the Paul Wurth Chair, University of Luxembourg. He obtained his PhD in 2019 from Imperial College London, United Kingdom. Afterwards, he worked in Prof. Kang Li's research group in the same department before moving to Germany in 2021 as an Alexander von Humboldt Research Fellow at the Institute of Functional Interfaces (IFG), Karlsruhe Institute of Technology (KIT). His research interest revolves around the development of porous materials particularly metal organic frameworks (MOFs) and their applications in the field of separation in particular membrane and adsorption.

2. Gas transport in mixed matrix membranes

Gas transport in the membrane-based hydrogen separation process can occur through different mechanisms. As illustrated in Fig. 1, the mechanisms can generally be classified based on membrane types, namely porous and dense membranes. In porous membranes, which are mainly fabricated using microporous materials,[4] the gas transport process can be further differentiated depending on the pore size of the porous membrane. At a molecular level where the membrane pore size is within the range of 0.5–10 nm, the molecular sieving phenomenon might govern the gas transport process. In this case, only gas molecules with a certain size can pass through the

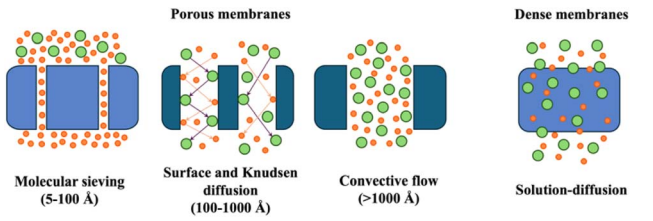

Fig. 1 The gas transport mechanisms in both porous and dense membranes.

membrane. As the pores of the porous membrane get bigger, surface and Knudsen diffusion might also play a role during the gas permeation process. Lastly, convective flow might also occur in such a porous membrane where the pore size is about 100 nm. This last case usually happens in a defective porous membrane. For hydrogen separation, the kinetic diameter of the hydrogen molecule, namely 0.289 nm, can then be used as a benchmark to fabricate porous membranes to ensure that the separation process occurs mainly through the molecular sieving mechanism.

Differing from porous membranes, in dense membranes, the gas transport mechanism occurs mainly through a solution-diffusion mechanism. In this case, gas molecules are first adsorbed on the surface of the membranes and then diffuse across the membrane before being desorbed at the permeate side of the membrane. This mechanism also applies for most of the MMMs since they are usually produced as dense membranes.

However, it should be noted that this gas transport process occurs only in an ideal scenario where the membranes contain no defective sites. As illustrated in Fig. 2, such a condition only occurs where a perfect interface can be established between fillers and the polymer. However, in most cases, some non-ideal cases might also occur in MMMs which can be classified into four different types: (i) particle agglomeration, (ii) interfacial void, (iii) polymer rigidification, and (iv) pore blockage. In the first non-ideal case, imperfection happens because of filler agglomeration which leads to the uneven distribution of fillers across the polymer matrix. Meanwhile, in the non-ideal case of (ii) to (iv), imperfection happens at the filler-polymer interface. Such imperfection can first lead to the establishment of the void at the filler-polymer interface (second case). Moreover, the imperfection at this filler-polymer interface might also result in the filling of this interface with rigidified polymeric chains (third case) or other compounds (fourth case) which might block the passage of the gas molecules to the fillers.

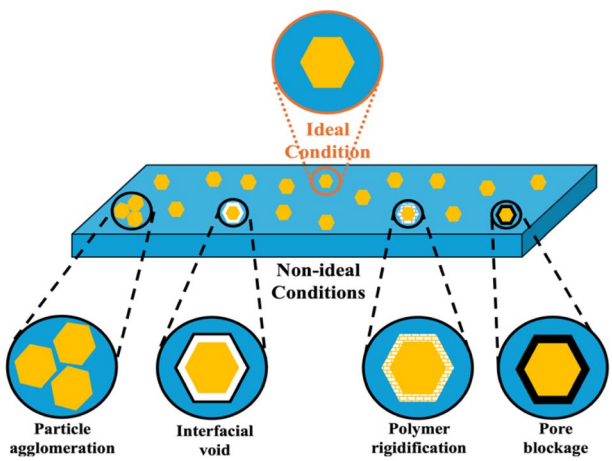

Fig. 2 An illustration of both ideal and non-ideal conditions that could occur in a MMM.

2.1 Gas transport models of ideal mixed matrix membranes

In general, four different types of gas transport models exist that can be used to describe the transport in a MMM: Maxwell, Bruggeman, Lewis-Nielson, and Pal. Each of these models will then be briefly explained below.

2.1.1 Maxwell model. In the field of MMMs, the Maxwell model serves as the basic model for predicting gas permeation in MMMs and was developed by Maxwell *et al.*[5] This model was initially developed in 1873 for estimating the dielectric properties of composite materials. Afterwards, because of the versatility of this model, it is used for predicting MMM permeation.[6] However, it should be noted that the applicability of this model is limited to ideal situations at low-loading MMMs with minimal particle interaction. The Maxwell model can then be defined with different expressions as shown in eqn (1):

$$\begin{aligned} P_{\text{eff}} &= P_{\text{c}}\frac{P_{\text{d}}+2P_{\text{c}}-2\phi_{\text{d}}(P_{\text{c}}-P_{\text{d}})}{P_{\text{d}}+2P_{\text{c}}+\phi_{\text{d}}(P_{\text{c}}-P_{\text{d}})} \\ &= P_{\text{c}}\frac{2(1-\phi_{\text{d}})+\alpha(1+2\phi_{\text{d}})}{(2+\phi_{\text{d}})+\alpha(1-\phi_{\text{d}})} \\ &= P_{\text{c}}\frac{1+2\phi_{\text{d}}(\alpha-1)/(\alpha+2)}{1-\phi_{\text{d}}(\alpha-1)/(\alpha+2)} \end{aligned} \tag{1}$$

where P_{eff} is the effective steady-state permeability of a gas molecule through a MMM, P_{c} is the continuous phase permeability, P_{d} is the dispersed phase permeability, and ϕ_{d} is the volume fraction of the dispersed phase. The Maxwell model can only be applied to suspensions of spherical particles with a volume fraction of filler particles below 0.2. In the case of higher volume fractions of filler particles, permeability cannot be predicted. According to this model, there are no defects or distortions in this MMM morphology case.

2.1.2 Bruggeman model. The limitation encountered in the Maxwell model regarding its applicability on low-loading MMMs is then addressed using the Bruggeman model which can account for MMMs with higher filler volume fractions.[7] The Bruggeman model was initially formulated for the electric constant of particulate composites and was modified to evaluate the performance of MMMs.[6] The model can be described in eqn (2) and (3) as shown below:

$$(P_{\text{r}})^{1/3}\left(\frac{\alpha-1}{\alpha-1}\right) = (1-\phi_{\text{d}})^{-1} \tag{2}$$

$$P_{\text{r}} = \frac{P_{\text{eff}}}{P_{\text{c}}} \tag{3}$$

Even though the Bruggeman model is an improved version of the Maxwell model, it still has the same limitations as the Maxwell model, namely ideal homogeneity assumption, simplified fillers' geometry and alignment, and neglect of interfacial defects between fillers and polymers. Furthermore, it needs to be solved numerically since it is an implicit equation.

2.1.3 Lewis-Nielson model. Another model that can be used to predict the MMM performance is the Lewis-Nielsen model which was originally developed for an elastic modulus of particulate composites.[8] The Lewis-Nielsen model improves

predictive accuracy by incorporating particle morphology effects, making it suitable for a wider range of conditions.[6] Even though it faces challenges with mathematical divergence at extreme permeability ratios, this model is still useful to predict the effective permeability of MMMs and this model can be expressed using eqn (4) and (5) below:

$$P_r = \frac{P_{eff}}{P_c} = \frac{1 + 2\phi_d(\alpha - 1)/(\alpha + 2)}{1 - \Psi\phi_d(\alpha - 1)/(\alpha + 2)} \quad (4)$$

$$\Psi = 1 + \left(\frac{1 - \phi_m}{\phi_m^2}\right)\phi_d \quad (5)$$

The computation of this model is simple, and it may accurately depict permeability behavior within the $0 < \phi_d < \phi_m$ range by taking into account the impact of particle morphology on permeability. Also, it can be reduced to the Maxwell model when ϕ_m approaches 1 ($\phi_m \rightarrow 1$). The relative permeability at $\phi_d = \phi_m$ is found to be diverging when the permeability ratio approaches infinity ($\alpha \rightarrow \infty$).

2.1.4 Pal model. Lastly, the MMM performance can also be predicted using the Pal model that was initially applied for the thermal conductivity of particulate composites while it was adjusted to predict permeability afterward.[9] In comparison to the rest of the models, the Pal model could be considered the most comprehensive which accounts for filler packing effects and can be applied across broader filler volume fractions.[6] This model can be expressed using eqn (6) as expressed below:

$$(P_r)^{1/3}\left(\frac{\alpha - 1}{\alpha - P_r}\right) = \left(1 - \frac{\phi_d}{\phi_m}\right)^{-\phi_m} \quad (6)$$

Same as the Lewis–Nielsen model, this model also covers MMM filler loading of $0 < \phi_d < \phi_m$ and considers the membrane morphology. On the other hand, the equation is implicit and requires being solved numerically like in the Bruggeman model.

The summary of gas transport models that can be used to predict the MMM performance, together with their respective strengths and weaknesses, is then given in Table 1.

2.2 Gas transport models of non-ideal mixed matrix membranes

In non-ideal MMMs, interfacial defects impact the membrane's performance; thus, these defects must be considered in predicting models. As mentioned previously, these interfacial defects include sieve-in-a-cage, matrix rigidification, plugged sieves (fillers), and leaky interfaces. These defects occur on the interface between the filler and polymer matrix, known as the interphase.

Several models have been developed for predicting the performance of nonideal MMMs. However, the model developed by Li *et al.* demonstrates the prediction in a simple way.[10,11] In this model, the basic Maxwell model is modified in a way to consider matrix rigidification and filler pore blockage at the same time. This model assumes that MMMs comprise two pseudo-dispersed phases. Therefore, the Maxwell model was applied three times to reach overall permeability. The first pseudo phase is composed of a dispersed phase combined with the interface skin affected by the plugged filler, and the second pseudo phase includes the first phase (considered a dispersed phase) together with the rigidified polymer matrix. Initially, the calculation began with the first pseudo phase permeability equation as shown in eqn (7).

$$P_{ps1} = P_{blo}\left[\frac{P_d + 2P_{blo} - 2\phi_{ps1}(P_{blo} - P_d)}{P_d + 2P_{blo} + \phi_{ps1}(P_{blo} - P_d)}\right] \quad (7)$$

where P_{ps1} is the first pseudo phase permeability, P_{blo} is the permeability of the interface layer affected by the plugged filler, P_d is the filler permeability, and ϕ_{ps1} is the volume fraction of the filler in the first phase. The ϕ_{ps1} is calculatable with eqn (8):

$$\phi_{ps1} = \frac{\phi_d}{\phi_d + \phi_{blo}} \quad (8)$$

Table 1 Summary of the gas transport models for ideal MMMs

	Scope	Strengths	Limitations
Maxwell	Effective for low filler volume fractions ($\phi_d < 0.2$) in dilute suspensions of spherical particles	Simple and widely accepted; assumes ideal morphology without defects or distortions	Cannot predict permeability at higher filler volume fractions due to interactions between particles
Bruggeman	Extends applicability to larger ranges of filler volume fractions compared to the Maxwell model	Considers random dispersion of particles; improves predictions for higher ϕ_d	Still shares some limitations of the Maxwell model; requires numerical solutions due to an implicit function
Lewis-Nielson	Covers permeability prediction for $0 < \phi_d < \phi_m$, considering particle morphology effects	Represents more accurate permeability behavior by incorporating morphology effects; reduces to the Maxwell model when $\phi_m \rightarrow 1$	Shows divergence in relative permeability (P_{eff}) at $\phi_d = \phi_m$ when the permeability ratio (α) tends to infinity
Pal	Covers $0 < \phi_d < \phi_m$, incorporating filler packing difficulties and morphology effects	Extends applicability to wide ranges of ϕ_d in ideal morphologies (two-phase systems without defects or distortions). Reduces to the Bruggeman model when $\phi_m \rightarrow 1$	Requires numerical solutions; shares similarities with the Bruggeman model in its numerical complexity

Table 2 Summary of various models used to predict the hydrogen separation performance of MMMs

Filler	Polymer	Filler loading (wt%)	Prediction models	Comment
ZIF-90 (ref. 15)	6FDA-triptycene	50	Maxwell and Bruggeman	The Maxwell model matches better with experimental data than the Bruggeman model
ZIF-8 (ref. 16)	Thermally rearranged hydroxyl polyimide	20	Maxwell	The Maxwell model demonstrates that interfacial voids disappear with thermal treatment
ZIF-8-polydopamine[13]	Troger's base polymer	40–50	Maxwell	The Maxwell model matches experimental data. The selectivity value is higher in the experiment than in the prediction due to pore modification caused by polydopamine
ZIF-8 (ref. 12)	6FDA-Durene	33.3	Maxwell	Experimental selectivity matches the Maxwell model. Experimental permeabilities are higher than those of the Maxwell model, attributed to enhanced polymer free volume with the addition of the filler and agglomeration of some filler nanoparticles
HKUST-1 (ref. 17)	Cyclic olefin copolymer	40	Maxwell, Maxwell–Wagner–Sillars, Bruggeman, Pal, Lewis-Nielsen and Higuchi	Experimental permeabilities follow the Higuchi model. It deviated negatively from other models due to immobility of polymer chains due to high T_g, pore blockage with rigid polymer layers, low driving forces from the permeability test at 1 atm, and enhanced filler-polymer interfacial interaction
ZIF-7 (ref. 18)	Polybenzimidazole	20–50	Maxwell	Experimental permeabilities are higher than predicted permeabilities. This is attributed to good interaction between the filler and polymer, increased T_g due to interfacial interaction and chain rigidification, and an increase in the free volume and higher pore size with increasing filler loading
ZIF-8 (ref. 19) and ZIF-90 (ref. 19)	Matrimid 5218	25	Maxwell	Experimental permeabilities are lower than the predicted ones. The Maxwell model overestimates the effect of ZIF-8 and ZIF-90 on permeability
ZIF-8 (ref. 20)	6FDA-BI	20	Maxwell	Predicted permeabilities match the experimental ones when the filler volume fraction is less than 27%, which demonstrates good filler-polymer compatibility
Pd@ZIF-67 gel[21]	PIM-1	28	Lewis-Nielsen	Predicted permeability is higher than experimental permeability. The Lewis-Nielsen model overestimates the effect of the filler on permeability. However, on increasing the filler amount, the deviation between predicted and experimental values decreases, which demonstrates the formation of interconnected networks within the fillers
Zeolite 13X,[22] ZSM-5,[22] and zeolite 4A[22]	Matrimid 5218	20–30	Maxwell	Experimental permeabilities are higher than the predicted ones, except for H_2 and N_2 permeabilities of zeolite 4A-based MMMs. This demonstrates the poor filler-polymer interfacial adhesion and interfacial voids
Sodalite[23]	Polyetherimide	10	Maxwell	The experimental values are higher than the predicted ones. This is caused by the low permeability of the pure sodalite membrane, which stems from its small crystal size, longer diffusion paths, and higher diffusion resistance. Additionally, small voids affected the accuracy of the Maxwell model
GO[14]	Pebax	0.01–0.04	Maxwell	There was a big deviation between the experimental and predicted values. The Maxwell model could not predict the transport properties
Pd nanoparticles[24]	Polybenzimidazole	58	Maxwell	The predicted values match the experimental ones at 200 and 250 °C. There is a deviation below 200 °C, which the Maxwell model slightly overestimates

where ϕ_d is the volume fraction of the filler in the membrane and ϕ_{blo} is the volume fraction of the interface layer affected by the plugged filler in the membrane. Moreover, the permeability of the second pseudo phase (P_{ps2}) determined with eqn (9):

$$P_{ps2} = P_{rig}\left[\frac{P_{blo} + 2P_{rig} - 2\phi_{ps2}(P_{rig} - P_{ps1})}{P_{ps1} + 2P_{rig} + \phi_{ps2}(P_{rig} - P_{ps1})}\right] \quad (9)$$

where P_{rig} is the rigidification region permeability and ϕ_{ps2} is the volume fraction of the first pseudo phase in the second pseudo phase. The ϕ_{ps2} can be calculated using eqn (10) as shown below:

$$\phi_{ps1} = \frac{\phi_d + \phi_{blo}}{\phi_d + \phi_{blo} + \phi_{rig}} \quad (10)$$

where ϕ_{rig} is the volume fraction of the rigidified region in the membrane. Ultimately, the overall permeability of the MMM can be calculated by using the Maxwell model for the third time by considering the polymer matrix as the continuous phase and the second pseudo phase as the dispersed phase and the final eqn (11) is given below:

$$P_{MMM} = P_c\left[\frac{P_{ps2} + 2P_c - 2(\phi_d + \phi_{blo} + \phi_{rig})(P_c - P_{ps2})}{P_{ps2} + 2P_c + (\phi_d + \phi_{blo} + \phi_{rig})(P_c - P_{ps2})}\right] \quad (11)$$

where P_{MMM} is the MMM's overall permeability and P_c is the polymer matrix's permeability.

Having extensively discussed the various models that can be used to predict the gas separation performance in MMMs, the summary of the models that have been practically used to describe the performance of MMMs for hydrogen separation is given in Table 2. From the summary, it can be seen that the Maxwell model appears to be the most commonly used model to predict the hydrogen separation performance of MMMs. It is frequently chosen due to its simplicity and generally good agreement with experimental data, especially in systems where the filler and polymer exhibit strong interfacial compatibility. However, filler loading has a significant impact on the Maxwell model predictive accuracy. At moderate to high filler loadings (*e.g.*, 40–50 wt%), the model sometimes overestimates permeability or selectivity due to factors such as filler agglomeration, pore modification, or increased free volume in the polymer matrix as exemplified in the cases of MMMs loaded with ZIF-8.[12,13] Similarly, at low filler loadings, as exemplified in the case of MMMs loaded with graphene oxide,[14] large deviations from predicted values are also noted, indicating the model's limitations in capturing transport behaviour when the filler influence is minimal or interfacial voids dominate. Other models such as Lewis-Nielsen and Higuchi have also been applied in cases involving high filler loading or rigid polymers, with the Higuchi model having better prediction due to reasons such as hindered polymer chain mobility and enhanced filler-polymer interactions. Overall, while the Maxwell model remains a valuable tool, it might not be very accurate to predict MMMs with both very low and high filler loading. Therefore, prediction of hydrogen gas separation performance of MMMs requires careful consideration of filler loading (in case the Maxwell model is used, filler loading must be below 30%) and its impact on the membrane's structure and polymer–filler interaction.

3. Mixed matrix membranes for hydrogen separation: filler criteria and fabrication strategies

3.1 Filler criteria

In general, fillers that will be used as the discrete phase in MMMs must be able to be homogeneously dispersed in the chosen polymeric matrix. Therefore, the use of fillers with smaller particle sizes is better since this can avoid the issue of filler agglomeration. In addition to the particle size, it has also been observed that the filler geometry could also play an important role in determining the hydrogen separation performance of MMMs. For instance, in a study involving three different $[Cu_2(ndc)_2(dabco)]$ MOF morphologies, namely bulk crystals, nanocrystals, and nanosheets, it has been observed that even though all of the fillers can improve the H_2 permeability of the bare membrane from around 3.6 to 5–6 Barrer, there is a significant difference regarding the improvement of the H_2/CO_2 selectivity.[25] At the same particle loading (20 wt%), the H_2/CO_2 separation performance of the bulk crystal-, nanocrystal- and nanosheet-based MMMs increases to be around 11, 14.7, and 15.7, respectively, from around 9.1 observed in the bare polymeric membrane. The same trend is also observed when using MUF-15 MOF crystals and nanosheets as fillers in a PIM-1 polymeric matrix. At 5 wt% loading, although both MMMs can elevate the H_2 permeability to be around 5000 Barrer, an improvement of H_2/N_2 selectivity of around 8% only occurs in the MMM fabricated using MUF-15 nanosheets as the filler while a decreasing trend is observed in the MMM fabricated using the bulk crystals as the filler.[26] This might then be attributed to the better filler-polymer compatibility as the particle size decreases, thereby promoting their uniform distribution across the polymer matrix.[25]

However, there is also a case where the use of nanosheet morphology is not preferable as exemplified in the study using MOF UZAR S-13 as the filler.[27] In this investigation, it has been shown that the use of spherical particles is preferable to nanosheets. The H_2/CH_4 selectivity of the MMM loaded with spherical nanoparticles and nanosheets is found to be around 13 and 9, respectively, which corresponds to an increase of around 76% and 24%, respectively. In this case, the better performance observed in the MMM loaded with spherical nanoparticles could be attributed to the presence of the amorphous phase that is more abundant in the spherical than in the nanosheet UZAR S-13. This leads to a more prominent decrease of CH_4 permeability found in the MMM loaded with spherical than nanosheet UZAR S-13, thus resulting in a higher selectivity improvement. This then shows that the selection of the filler morphology in MMMs could not be generalized and needs to be investigated individually depending upon the filler-polymer combination.

Moreover, in the field of MMMs for hydrogen separation, in addition to the particle size and morphology, it is also

important to select fillers with suitable pore sizes since this is related to the improvement of the molecular sieving properties of MMMs. Failing to meet this important criterion might then result in bare separation improvement in the resulting MMM. For example, in a study involving zeolite 5A using polysulfone-acrylate as the polymer matrix, it has been observed that barely any H_2/CO_2 separation improvement can be seen even though the polymer has been loaded with 40 wt% of the filler.[28] A similar trend has also been observed in a MMM fabricated using Matrimid as the polymer matrix loaded with Zeolite 13X and ZSM-5 as fillers, whose pore sizes fall around 0.74 nm and 0.55 nm, respectively.[29] At around 20–30 wt% particle loading, an improvement can only be seen in the H_2 permeability of the MMM where it increases from around 15 to 40 Barrer. However, both H_2/CO_2 and H_2/N_2 selectivity of both membranes decreased from 77.1 to 75 and from 4 to 2.3, respectively, in zeolite 13X/Matrimid and from 77.1 to 67.5 and 1.9, respectively, in ZSM-5/Matrimid. Such a similar tendency can also be seen with other fillers such as MOFs. By incorporating UiO-66-NH_2 with a pore size around 0.7 nm as the filler inside three different polymers, namely 6FDA-DAM, 6FDA-DAM : DABA (3 : 2), and 6BPDA-DAM (1 : 1), the only parameter that can be improved is H_2 permeability which increases around 3–4 times compared with the bare polymers.[30] However, their selectivity against various light gases (CO_2, N_2, and CH_4) can be barely improved even after the polymers are loaded with 40 wt% fillers.

Therefore, considering the molecular size of hydrogen, it could be first suggested to use a filler with a pore aperture around 3 nm. For example, Sigma-1 DDR zeolite has pore size around 0.36 × 0.44 nm which makes it suitable for H_2 separation from other light gases. This has been indicated based on the gas adsorption at 8 bar where the amount of H_2 and CH_4 adsorbed is found to be around 3.5 and 1 mol kg^{-1}, respectively.[31] In another study using ZIF-8 with a pore aperture around 0.34 nm, for example, even though the H_2/CO_2 selectivity of the MMM can only be slightly enhanced from 3 to 3.82 as the filler loading increases from 0 to 50 wt%, its H_2/CH_4 selectivity can be significantly improved from around 121 to 472.[32]

3.2 Fabrication strategies

Once an appropriate filler has been selected, a MMM for hydrogen separation can be fabricated. A MMM can usually be fabricated by mixing two different components, namely fillers and polymers. In a typical fabrication method, both components are initially combined to form a homogeneous suspension. Afterward, this suspension can be cast to form a membrane. The possibility of using other methods apart from casting, such as electrospinning[33] or melt processing,[34] has also been demonstrated to form MMMs.

Despite the conceptual simplicity of MMMs, namely the combination of fillers and polymers, the fabrication process to produce a defect-free MMM is not very straightforward. This is because a number of criteria need to be fulfilled in order to produce a defect-free MMM such as the absence of filler agglomerates to ensure even distribution of fillers in the polymer matrix and good compatibility between the filler and the polymer to avoid the generation of filler-polymer interfacial defects.[35]

Therefore, some process improvements can be introduced during the fabrication process of MMMs with the main aim of obtaining a defect-free MMM. Such improvements are particularly important to improve the interaction at the filler-polymer interfaces. One of the common strategies to address this issue is to do a priming process during the MMM fabrication. When a MMM is fabricated using a priming process, the polymer is added gradually when preparing the suspension. The rationale behind this step is to initially cover the surface of the fillers with a fraction of the polymer. It is expected that, by first covering the filler surface with the polymer, an enhanced interaction can be more easily established between the polymer and the filler resulting in a defect-free MMM. In addition to priming, the filler-polymer interaction can also be improved by introducing an external agent such as a chelating agent. For example, the use of zinc ions as a chelating agent has been observed for being able to improve the interaction between ZIF-8 and 6FDA-BI by acting as a bridge between the imidazole groups present in both materials.[36]

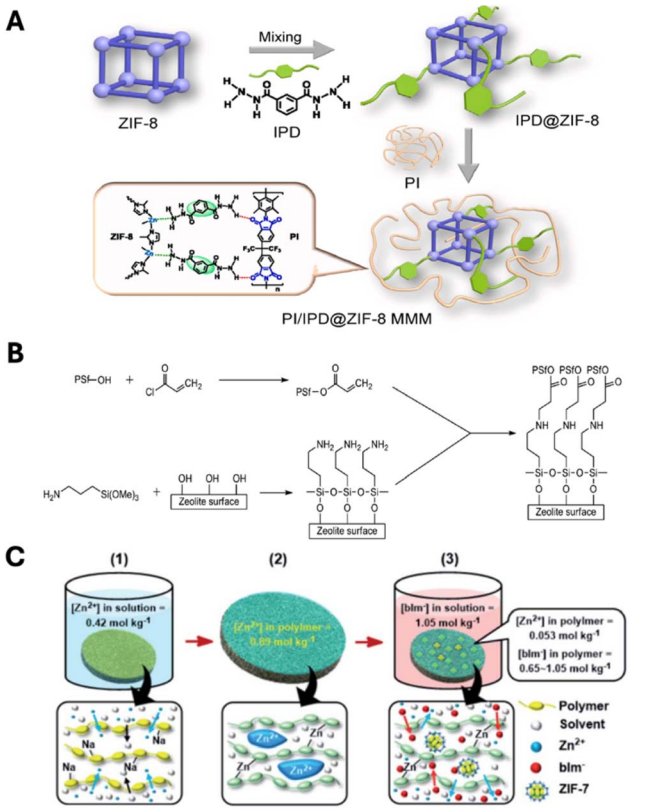

Fig. 3 Illustrations of various modification strategies to fabricate MMMs for hydrogen separation: isophthalic dihydrazide (IPD) coating on the surface of ZIF-8 (A), aminopropyltrimethoxysilane-modified zeolite-A in combination with acrylate-functionalized polysulfone (B) and the polymer-modification-enabled *in situ* MOF (PMMOF) method (C). Figures (A)[38] and (B)[28] are reproduced with permission. Copyright 2021 and 2010, respectively, Elsevier. Figure (C) is reproduced with permission.[44] Copyright 2020, Royal Society of Chemistry.

Another common strategy that can be used to improve the interaction between both components in MMMs is through filler modification. For example, growing $Mg(OH)_2$ nanostructures on silica nanoparticles has been observed to be able to reduce the solvent–particle interaction during the MMM fabrication process, thus increasing the tendency for the silica nanoparticles to get adhered onto the polymer matrix.[37] A similar strategy can also be used with MOF-based MMMs such as by coating isophthalic dihydrazide (IPD) on ZIF-8, as illustrated in Fig. 3(A),[38] ethylenediamine on ZIF-90 (ref. 39) and (poly)dopamine on ZIF-8.[40–42] In particular with MOFs, this strategy can also be realized through a mixed ligand strategy where some portions of the default MOF's ligand are replaced by other ligands. This has been shown, for example, in a mixed-ligand ZIF-8 where some of the methylimidazole is replaced with 2-aminobenzimidazole to improve the interaction with the Torlon polymer.[43]

Moreover, it is possible to modify not only the filler but also the polymer to further enhance the interaction of both components. As illustrated in Fig. 3(B), this approach has been studied, for example, in the case of a zeolite 3A/polysulfone-acrylate MMM.[28] In this case, the modification of both the filler and the polymer is carried out by functionalizing the zeolite surface with aminopropyltrimethoxysilane (APTMS) and the introduction of an acrylate functional group in the polymer to build a covalent bond between the zeolite and the modified polymer. In another investigation using a ZIF-8-90/6FDA-DAM:DABA MMM, the modification is carried out through a mixed ligand strategy for the MOF and by introducing more COOH groups in the polymer to increase the number of hydrogen bonding sites in the MMM.[44] By employing the same strategy—using the mixed-ligand ZIF-8-NH_2 and a benzimidazole-containing polyimide—the enhanced interaction arises from hydrogen bonding between the amino ligands and the carboxylic moieties in the polymer and from π–π stacking interactions between the benzimidazole moieties present in both the MOF and the polymer.[45]

In addition to the filler modification, the *in situ* technique can also be used as an effective strategy for MMMs for hydrogen separation. As the name suggests, this strategy usually involves the synthesis of fillers during the membrane fabrication process. In this case, differing from the conventional fabrication method, the fillers are not separately prepared before the MMM fabrication, but they are synthesized during the MMM fabrication. One of the key advantages of using this method is the possibility of reducing filler-polymer interfacial defects. In other words, the fabrication process is not initiated by two heterogeneous phases which can cause a defect.

One example where this method is implemented can be seen in the fabrication of a ZIF-7 MMM, as illustrated in Fig. 3(C).[44] In the study, the fabrication process of the MMM is initialized by first forming a polymeric thin film of 6FDA-DAM followed by four main steps: (i) hydrolysis with sodium formate, (ii) ion exchange between sodium and zinc, (iii) ligand treatment and (iv) imidization. In this case, the propensity of the interfacial defect formation between the filler and the polymer could be reduced because the zinc ions, which are the precursor for ZIF-7, have been first embedded through an ion-exchange process within the polymeric chains. In addition, the confined space within the polymeric chains has also suppressed the particle growth, thus enabling the formation of nano-sized ZIF-7 which is more suitable for thin-film membrane formation.

Lastly, a stronger interaction between the filler and the polymer can also be established by cross-linking the filler and the polymer. This approach has been studied to produce MMMs involving MIL-53(Al)–NH_2 with polyimide for hydrogen separation.[47] In this study, first, the filler is mixed with the polyimide precursor, namely polyamic acid. The main objective of this approach is to build hydrogen bonds between the amine group of the MOF and the carbonyl group of the polyamic acid. Upon imidization, an additional amide bond can also be established between the amine and the carboxylic acid group. In this case, the cross-linking process occurs through the establishment of both the hydrogen and amide bonds.

The effectiveness of these strategies can usually be observed by the successful fabrication of MMMs with very high particle loading without any indication of large interfacial defects. Additionally, these strategies enable an increase in gas separation performance that cannot be achieved in other scenarios.[38,40,44] For example, up to 50 wt% polydopamine-coated ZIF-8 can be loaded in the Troger's base polymer without any indication of reduction in gas selectivity.[40] In another study using a ZIF-8-90/6FDA-DAM:DABA MMM, around 12.1% of H_2/CH_4 selectivity enhancement to be around 75 was observed with a MMM fabricated using a modified polymer with enhanced COOH groups while the MMM fabricated using the unmodified polymer shows a declining selectivity trend.[44]

4. Fillers in mixed matrix membranes for hydrogen separation

4.1 Zeolites

In the field of MMMs, zeolites are one of the first fillers used to improve the separation performance of polymeric membranes. In the case of hydrogen separation, a number of zeolites such as hollow zeolite spheres (HZSs),[37] Sigma-1 DDR,[31] sodalite,[48,49] zeolite 13X,[29] zeolite 3A,[28] zeolite 4A,[29,50–52] zeolite 5A,[28] ZSM-5 (ref. 29) and zeolite-Y[53] have been investigated as fillers in MMMs.

Because of their well-defined pore size, when a zeolite with a suitable pore size has been chosen and can be successfully incorporated inside a polymer matrix without generating any defects, one can then expect a significant hydrogen separation performance improvement which is mainly attributed to the improvement of the hydrogen molecular sieving capability. For instance, the pore size of DDR and sodalite, which falls around 0.36 × 0.44 nm and 0.28 nm,[31,49] respectively, enables the H_2 molecule to easily penetrate the zeolite pore while preventing larger gases from passing through their pores and thus increasing the MMM selectivity. In the case of a DDR/Matrimid MMM, as illustrated in Fig. 4(A and B), loading the polymer with 22 wt% of zeolite can increase both the H_2 permeability and H_2/CH_4 selectivity from around 17 to 35 and from 130 to 375,

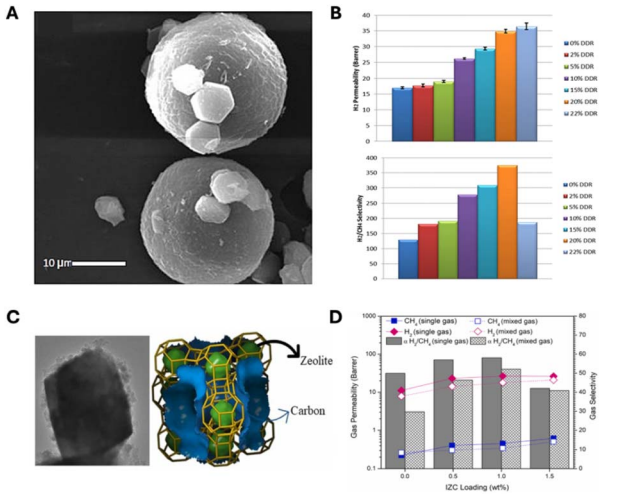

Fig. 4 Micrograph images of DDR zeolite (A) and carbon-impregnated zeolite-Y (C). The hydrogen separation performance of DDR Zeolite/Matrimid (B) and carbon-impregnated zeolite(Y)/P84 (D) at different particle loadings. Figures (A and B)[31] and (C and D)[53] are reproduced with permission. Copyright 2017 and 2024, respectively, Elsevier.

respectively.[31] Similarly, the H_2/N_2 separation performance of the polyetherimide that is loaded with 10 wt% of nanosized sodalite can also be improved almost 4 times from around 4.3 to 16.9 while the H_2 permeability also significantly increases from around 13.5 to 7155 Barrer.[49] An improvement in molecular sieving has also been observed when the zeolite is combined with rubbery polymers such as PDMS, where a reversal in the hydrogen selectivity trend occurs.[50] In the neat PDMS membrane, the H_2 permeability and H_2/CH_4 selectivity are found to be around 1313 Barrer and 0.8, respectively. Higher CH_4 permeability is caused since it is more condensable than H_2. Once loaded with 40 wt% of zeolite 4A, the H_2 permeability and H_2/CH_4 selectivity can be improved to 9516 Barrer and 8.7, respectively. All these cases highlight the importance of using zeolites with a suitable pore size to improve the molecular sieving performance of MMMs.

Selecting zeolites with a suitable pore size is not the only strategy to improve the hydrogen molecular sieving capability of MMMs. Another strategy that can be used is by modifying the pores of the zeolite. This has been studied by impregnating the zeolite-Y pore with carbon structures using sucrose as the carbon source, as illustrated in Fig. 4(C and D).[53] As expected, this process can significantly reduce the surface area of the zeolite around 5 times to be around 133 $m^2 g^{-1}$. Despite this negative impact, both the hydrogen permeability and selectivity of the MMM that is loaded with 1 wt% of the impregnated zeolite can be simultaneously enhanced. The H_2 permeability increases from around 11 to 27 Barrer while the H_2 selectivity against N_2 and CH_4 goes up from around 51 to 59 and 50 to 58, respectively. Such performance enhancement cannot be observed when the MMM is loaded with non-modified zeolite-Y which is caused by the combination of poor membrane-filler compatibility and the lack of molecular sieving properties.

4.2 Graphite- and graphene-based materials

In addition to zeolites, another class of inorganic materials that can be used as a filler in MMMs is graphite- and graphene-based materials. Graphene or graphene oxide, which is obtained through the exfoliation of graphite or graphite oxide, offers the advantages of reducing the thickness of MMMs due to their 2D morphology and atomically thin structure.[54] Therefore, few studies have investigated the incorporation of these materials into various polymers for hydrogen separation.[55–59] Also, few studies have indicated that incorporating graphite- or graphene-based fillers can indeed negatively impact the membrane permeability.[55,56] In an investigation using graphite oxide loaded in both polysulfone and polyimide, both the hydrogen permeability and selectivity decrease in the MMM which is caused by the increase in the diffusional barrier and difficulty in obtaining a MMM with good filler dispersion.[55] Using PEBAX as the polymer, it has been observed that the permeability of all the gases decreases after adding GO inside PEBAX because GO adds more barriers for the diffusional process of the gases.[56] However, around a 56% improvement in the H_2/CH_4 selectivity compared to bare PEBAX can still be observed because, as the smallest gas, H_2 experiences the least permeability reduction. Similarly, loaded with 0.1 wt% thermally reduced graphite oxide, although the H_2 permeability barely changes, both the H_2/N_2 and H_2/CH_4 selectivity can be increased from around 50 to 90.[58] In the same study, a slightly better performance can then be obtained by using chemically reduced graphite oxide, where a slight increase in H_2 permeability is observed from 22 to 24 Barrer. This is then accompanied by the improvement of H_2 selectivity against N_2 and CH_4 from around 50 to 110 and 230, respectively.

Moreover, there is also a possibility to modify these fillers with other materials. For instance, a hybrid material can be formed by combining GO with an ionic liquid.[57] Using this approach, at 0.5 wt% loading, even though the H_2 permeability of the MMM barely changes from that of the pure PEBAX membrane, more than a 50% improvement in the H_2/N_2 selectivity to around 6.8 has been observed.

4.3 Metal organic frameworks (MOFs)

One of the main disadvantages of using zeolites or graphene-based materials in MMMs for hydrogen separation is that they are purely inorganic, and this could pose a compatibility issue with some polymers. Therefore, recent advancements in porous materials have also shown the possibility to use other types of fillers in MMMs for hydrogen separation which are partially built from organic materials, which are called metal organic frameworks (MOF). As the name suggests, such porous materials are constructed using two different components: metal clusters, which serve as structural building units (SBUs), and organic ligands connecting the SBUs. Several types of MOFs such as CAU-1-NH_2,[60,61] CAU-21-ODB,[62] [Cu_2(ndc)$_2$(dabco)],[25] HKUST-1,[34] MIL-101(Cr),[63] MIL-101-NH_2,[64] MIL-101-$PhSO_3H$,[64] MIL-101-COOH,[64] MIL-53(Al),[34,65] MIL-53(Al)–NH_2,[47,61] MOF-5,[66] MOF-74(Mg),[65] MUF-15,[26] TIFSIX 3,[65] UiO-66,[55] UiO-66-NH_2,[30,63,67] UiO-66-$(OH)_2$,[68] UiO-66(Hf)–$(OH)_2$,[69] UZAR S-13,[27]

ZIF-L,[70,71] ZIF-7,[46,72–74] ZIF-8,[32,36,38–45,63,75–84] ZIF-11,[85–87] ZIF-12,[88] ZIF-67,[89] ZIF-90,[39,44,90] ZIF-93,[87] and $Zn_2(bim)_4$ (ref. 65) have then been investigated as fillers to improve the hydrogen separation performance of polymeric membranes. In addition, the potential of using other MOF-based materials such as post-synthetically modified MOFs,[74] MOF-based hybrid materials such as UiO-66-graphite oxide[55] and MOFs with mixed ligands such as mixed-ligand ZIF-8,[43] ZIF-8/90 (ref. 44) and ZIF-93/11 (ref. 87) has also been studied to enhance the gas separation performance of polymeric membranes.

As in the case of zeolites, the separation performance improvement in MOF-based MMMs can be primarily attributed to enhanced molecular sieving. This can be seen, for example, in ZIF-based MMMs considering that the pore aperture of most of the ZIF materials used in this case falls in the range between 0.3 and 0.4 nm.[32,44,46,72,73,75,79,80,86] In an investigation using polybenzimidazole as the polymer matrix which is loaded with 50 wt% of ZIF-7, an improvement in both the H_2 permeability and H_2/CO_2 selectivity can be clearly observed.[72] The H_2 permeability increases from 3.7 to 26.2 Barrer while the H_2/CO_2 selectivity can be enhanced from 8.7 to 14.9. The same trend is also observed when loading ZIF-7 in polyetherimide, where the H_2 permeability and H_2/CO_2 selectivity can be increased by around 35% to 65% to be around 9 Barrer and 8.4, respectively.[73] Using the *in situ* MMM fabrication method, layered ZIF-7 with a non-porous structure can also be obtained.[46] Even though the H_2 permeability in the MMM slightly decreases from the bare polymeric membrane from around 589 to 322 Barrer, its non-porous nature can have a more positive impact on the molecular sieving ability of the MMM. As a result, the H_2 selectivity against CO_2, N_2, and CH_4 increased from around 1.4 to 4.4, 30,6 to 59.5, and 40.2 to 172.2, respectively.

In another study, by loading the Matrimid polymer with 50 wt% ZIF-8, the H_2/CH_4 selectivity was significantly increased from around 121 to 472.[32] Despite this positive impact, this needs to be compromised by a slight reduction of H_2 permeability from around 29 to 18 Barrer, since adding ZIF-8 in a large fraction will also force the gas molecules to have a more tortuous path as they diffuse across the MMM. Meanwhile, such a case is not observed when combining ZIF-8 and polybenzimidazole since both the H_2 permeability and H_2/CO_2 can be simultaneously improved by about 28 times and 43%, respectively, to be around 105 Barrer and 12.3.[80] A similar trend can also be observed in a study using an asymmetric membrane fabricated from polysulfone loaded with 10 wt% ZIF-8.[77] In this case, both the H_2 permeability and selectivity against N_2 and CH_4 can be enhanced. The permeability improves from 40 to 87 Barrer while the H_2/N_2 and H_2/CH_4 selectivity increases from 45.6 to 65.9 and 45.5 to 63, respectively.

Improvement in molecular sieving can also be achieved by incorporating other ZIF materials such as ZIF-11 in the Matrimid polymer.[86] At 30 wt% particle loading, the H_2 permeability and H_2/CH_4 selectivity increase around 5 and 2 times, respectively, to be around 103 Barrer and 141, respectively. A similar performance improvement has also been observed when using ZIF-90 as the filler in 6FDA-DAM:DABA.[44] At 10 wt% particle loading, the H_2 permeability and H_2/CH_4 selectivity of the MMM can be improved to be around 219 Barrer and 71, respectively, from 156 Barrer and 61. Moreover, molecular sieving improvement can also be seen in ZIFs with mixed linkers such as ZIF-93/11.[87] Using this filler in polybenzimidazole, not only can the H_2 permeability be increased from around 50 to 207 Barrer, but its H_2/CO_2 selectivity also improves from around 4 to 7.7.

Improvement in molecular sieving in ZIF-based MMMs is also observed when using modified ZIFs.[38,43] For example, by using isophthalic dihydrazide-modified ZIF-8 and polyimide as a polymer, it has been observed that, at 45 wt% particle loading, both H_2 permeability and H_2/CH_4 selectivity of the bare polymer can be increased from 1534 to 7982 Barrer and 12.6 to 15.1, respectively.[38] Modification of ZIF-8 through a mixed ligand strategy by combining 2-methylimidazole and 2-aminobenzimidazole has also proven the capability to improve the hydrogen separation performance of the MMM through molecular sieving.[43,45] As illustrated in Fig. 5(A and B), using this mixed-ligand strategy, a MMM with an optimum loading of 16 wt% particle loading can be obtained. The result from the gas separation performance shows that the H_2 permeability of a bare Torlon membrane can be increased from around 1.8 to 4.92 Barrer. Meanwhile, both the H_2/N_2 and H_2/CH_4 selectivity can be improved by around 10 times from 24.3 to 278 and 31.5 to 302, respectively.[43] In this case, the realization of ZIF-8 molecular sieving in the MMM is enabled by the absence of interfacial defects thanks to its modification.[38,43,45]

The achievement of such a separation performance improvement is not only limited to ZIF-based MMMs but also has been observed by using aluminum-based MOFs.[47,60–62,91] The use of this type of MOF can also be more beneficial since they are constructed from higher valence atoms, thus providing a more robust framework.[91] In a study using CAU-1-NH_2 as the filler, whose pore aperture is around 0.3–0.4 nm, the H_2/CO_2 selectivity of the PMMA membrane increased from around 3 to 13.[60] This is also accompanied by an improvement in the H_2 permeability more than 2 times to around 11 100 Barrer. A similar trend can also be seen when loading PIM-1 with around 23 wt% of CAU-21-ODB, whose pore aperture is around 0.33 nm.[62] Considering its small pore size, the H_2/N_2 selectivity of the MMM can be significantly improved from around 8 to 39 which also goes hand in hand with around a 116% increase in H_2 permeability to be around 7300 Barrer. In another investigation involving MIL-53-NH_2, the H_2/CO_2 selectivity of the polyimide membrane was improved from around 6.5 to 44.6, which also goes hand in hand with more than a 3-fold increase in the H_2 permeance to be around 24×10^{-9} mol s^{-1} Pa^{-1} m^{-2}.[61] Using the same combination of MIL-53-NH_2 and polyimide fabricated using an *in situ* interfacial cross-linking approach, as illustrated in Fig. 5(C and D), at 30 wt% particle loading, the H_2 permeability and H_2/CO_2 selectivity of the polymer can be improved from around 10 to 384 Barrer and from around 6 to 17, respectively.[47] Moreover, almost no performance deterioration can be observed in this particular MMM for almost 2 weeks.

In addition to molecular sieving, the gas separation performance improvement can also be attributed to the impact coming from the increase of affinity or adsorption sites of MMMs towards hydrogen. For example, by loading ZIF-8 with

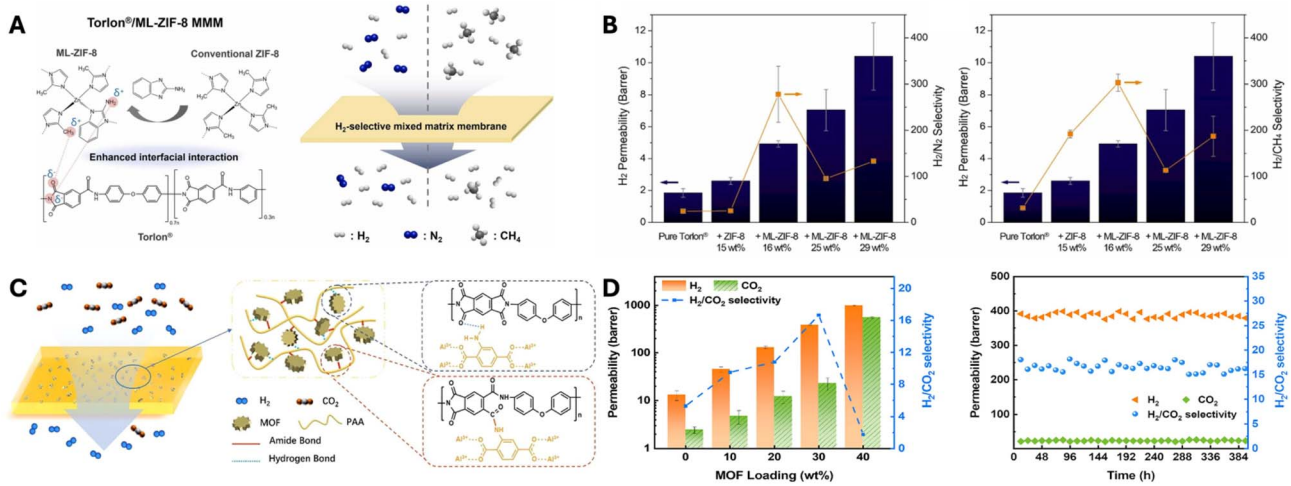

Fig. 5 Illustrations of MMMs using MOFs as fillers with their corresponding hydrogen separation performance exemplified in mixed-linker ZIF-8/Torlon (A and B) and *in situ* fabricated MIL-53(Al)/polyimide (C and D). Figures (A and B)[43] and (C and D)[47] are reproduced with permission. Copyright 2024 and 2023, respectively, Elsevier.

palladium, its adsorption and affinity towards H_2 can be significantly enhanced.[81] In this case, by using Matrimid as the polymer, the H_2 permeability of the bare polymeric membrane can be increased more than 2 times to be around 69 Barrer while the selectivity of H_2 against CO_2, N_2, and CH_4 also improves from around 2.9 to 5, 124.5 to 201.1 and 92.4 to 136, respectively.

Engineering adsorption sites can also be directed to other gases such as CO_2, which might be beneficial for H_2/CO_2 separation as exemplified in the case of MIL-101-NH_2/cellulose nanofiber,[64] ZIF-L/Polyimide[70] and ethylenediamine modified-ZIF-90/Matrimid[39] MMMs. Differing from the selectivity improvement contributed by molecular sieving, the improvement from the solubility selectivity might be correlated with the increase of the CO_2 adsorption sites in MOFs, thus hindering its permeability. For example, in the case of a ZIF-L MMM, adding the MOF into the polyimide will increase the CO_2 adsorption sites in the MMM.[70] In tandem with the small pore size of ZIF-L (0.31 nm), the incorporation of 20 wt% ZIF-L into polyimide increases the H_2/CO_2 selectivity from 1.8 to 13.4 which is also accompanied by around an 18% improvement of its H_2 permeability to be around 260 Barrer. However, almost no improvement in H_2/N_2 and H_2/CH_4 selectivity can be observed since ZIF-L does not provide additional adsorption sites for both N_2 and CH_4. In another investigation using UiO-66(Hf)–$(OH)_2$ embedded in polybenzimidazole, it was shown that the H_2/CO_2 selectivity can be increased from around 9.5 to 19.4.[69] In this case, the increase in H_2 permeability from around 3.6 to 8.1 Barrer does not go hand in hand with the trend of CO_2 permeability which barely goes up since the MOF has a stronger affinity towards CO_2 and thus could contribute to hindering its diffusional process across the MMM.

However, it should also be noted that the positive impact attributed to the incorporation of MOFs in polymers can also be reduced where they do not really become an integral part of the transport process. This can be exemplified in the case of a free-volume enlargement phenomenon of the polymer chain as studied in the case of a ZIF-8/PIM-1 MMM.[78] In this case, in the as-cast ZIF-8/PIM-1 film, an improvement in both H_2 permeability and selectivity can be clearly observed. The H_2 permeability increases from 1630 to 6680 Barrer accompanied by the simultaneous enhancement of H_2/N_2 and H_2/CH_4 selectivity from 9.1 to 19.1 and from 5.3 to 15.5, respectively. In contrast, in the ZIF-8/PIM-1 alcohol-treated MMM, even though the H_2 permeability can be significantly increased from 3300 to 14 430 Barrer, both the H_2/N_2 and H_2/CH_4 selectivity can only be barely enhanced from 6.6 to 8.2 and 4.5 to 5.4, respectively. As alcohol treatment of PIM-1 usually leads to an increase in the polymeric chain free volume, this might also lead to diversion of the gas transport in the MMM. In this case, the gas pathway through the MOF becomes less important and the gas will preferentially pass through both the increased free volume of the polymers and the interfacial cavities between polymers and fillers. Consequently, even though MMMs with higher permeability can be obtained, they will suffer from a significant decrease in selectivity.

4.4 Porous organic frameworks (POFs)

Hand in hand with the growing interest in the research and development of MOFs, there is growing interest in using another class of porous materials which are completely built from organic compounds that can generally be classified as porous organic frameworks (POFs).[92] Unlike MOFs or zeolites, since POFs are completely built from organic compounds, they might offer better interfacial compatibility with polymers and thus might be more suitable to be used as fillers in MMMs. One of the earliest POFs that has been investigated as a filler in MMMs is porous aromatic frameworks (PAFs). PAFs can be classified as porous solids whose structure is mainly constituted of aromatic building blocks.[93] Even though PAFs are usually considered amorphous materials, like their porous crystalline counterparts, namely MOFs and COFs, they are also highly

porous, with a high surface area and tailorable architecture. Because of these advantages, it could also be expected that the hydrogen separation performance of polymeric membranes can be improved by incorporating PAFs. For example, at 5 wt% PAF-1 particle loading, the H_2 permeability of a triptycene polymer of intrinsic microporosity (TPIM) can be increased from 1651 to 2907 Barrer.[94] This is also accompanied by the improvement of H_2 selectivity against N_2 and CH_4 from 19.5 to 27 and 16 to 24.2, respectively.

During the last decade, there has also been growing interest in the research and development of covalent organic frameworks (COFs), which were first synthesized in 2D form in 2005.[95] As the name suggests, COFs are built through strong covalent bonds. Therefore, COFs also have high chemical stability which makes them superior for use for gas separation in harsh environments. On the other hand, synthesizing a self-standing COF membrane is technically and economically challenging. Therefore, utilizing them as fillers with polymers to make MMMs is logical.[96,97]

In recent years, 2D COFs have attracted significant research interest in this field, although 3D COFs are also being actively explored. This might be caused by their fascinating properties such as their nanometer thickness and large amount of exposed surface area.[98] For example, one of the earliest studies was carried out by employing two 2D COFs, namely TpPa-1 and TpBD with pore apertures around 1.8 nm and 2.4 nm, respectively.[99] Using polybenzimidazole (PBI) as the polymer, both COFs can be incorporated up to 50 wt% in a MMM. For a 40 wt% TpPA-1/PBI MMM, the H_2 permeability can be increased up to 3 times from the pristine polymer to be around 18.8 Barrer. This is also accompanied by an increase in the H_2 selectivity against N_2 and CH_4 from around 69 to 79 and from around 155 to 165.5, respectively. However, such a simultaneous improvement cannot be observed in the case of 50% TpBD/PBI since an enhancement can only be seen in the H_2 permeability from around 6.2 to 42.5 Barrer. Meanwhile, its H_2 selectivity against N_2 and CH_4 slightly decreases from around 69 to 66 and 155.5 to 139.7, respectively. This could then be associated with the pore aperture of both COFs. Considering that TpBD has a larger pore aperture than TpPA-1, this COF is then more effective in significantly enhancing the H_2 permeability of the MMM with a slight sacrifice in the H_2 selectivity. Another investigation involving 2D COFs has also been carried out by using NUS-2 and NUS-3, whose interlayer distances and pore sizes are found to be 3.3 Å and 3.9 Å and 0.8 nm and 1.8 nm, respectively, as illustrated in Fig. 6. Both COFs are then incorporated into PBI and Poly(ether imide) (Ultem) to fabricate MMMs.[100] Among the four MMMs, only a NUS-2-incorporating PBI MMM resulted in increased H_2/CO_2 selectivity from 9.5 to 31.4 which is nearly a 230% improvement and also surpasses the Robeson upper bound. The enhancement could be mainly attributed to the selective gas sorption characteristic of NUS-2

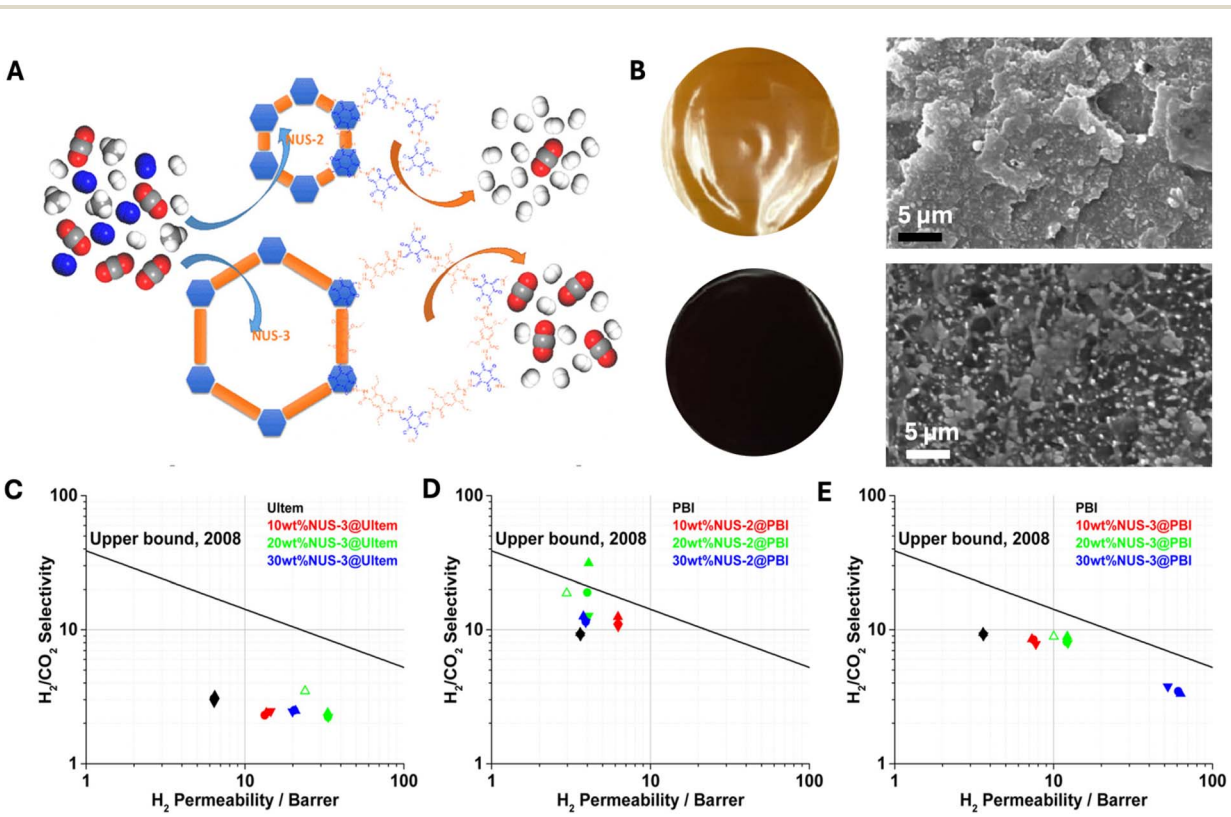

Fig. 6 Illustrations of the utilization of both COF NUS-2 and NUS-3 as fillers in MMMs for hydrogen separation: an illustration of both NUS-2 and NUS-3 showing their difference in pore aperture (A), photos and SEM micrographs of NUS-2 MMM (B, above) and NUS-3 MMM (B, below) and the hydrogen separation performance of the MMMs against Robeson upper bound (C–E). All figures are reproduced with permission.[100] Copyright 2016, American Chemical Society.

towards CO_2. This contrasts with the improvement of hydrogen separation performance in MMMs, which is usually attributed to the improvement in hydrogen molecular sieving or the improvement of the MMM affinity towards hydrogen. In this case, the relatively high affinity of NUS-2 towards CO_2 leads to the saturation of the COF pores with CO_2 under high pressure. Consequently, the CO_2 permeation across the MMM will be hindered, resulting in an overall decrease in CO_2 permeability. On the other hand, since the permeation of H_2 is relatively unhindered, the incorporation of NUS-2 adds more diffusional pathways, thus resulting in an increase in H_2 permeability. As a result, the H_2/CO_2 selectivity of the bare polymeric membranes can be improved once they are incorporated with NUS-2.

Lastly, another class of POFs that has been investigated as fillers in MMMs for hydrogen separation is hydrogen-bonded organic frameworks (HOFs). Unlike COFs, HOFs are porous solids that are built based on hydrogen bonds rather than covalent bonds. Since hydrogen bonding is weaker than either coordination or covalent bonding, HOFs are usually more flexible than MOFs or COFs. This flexible nature can equip HOFs with several advantages such as solution processability, ease of purification, and regeneration possibility. However, this flexibility also poses a challenge to obtain a HOF with a robust framework. Therefore, various strategies such as framework interpenetration and the establishment of π–π interaction can be utilized in tandem with hydrogen bonding to increase the robustness of HOFs and render HOFs more practicable for various applications including gas separation.[101–103] In this case, HOF-30 with a pore size of around 0.4 nm has been incorporated inside Matrimid.[104] At 10 wt% particle loading, the H_2 permeability increases from around 56 to 450 Barrer. Such an improvement also goes hand in hand with the enhancement of H_2 selectivity against CH_4 from around 23 to 62.

4.5 Others

Zeolites, graphite and graphene-based materials, MOFs and POFs are not the only materials studied as fillers to improve the hydrogen separation performance of MMMs. Another material that has been investigated as a filler in MMMs is silica nanoparticles. One study investigated the use of ordered mesoporous silica spheres (MSSs) as fillers in a 6FDA-DAM polymer for hydrogen separation.[37] At 16 wt% particle loading, the H_2 permeability and H_2/CH_4 selectivity were improved from 480 to 918 Barrer and from around 17 to 22, respectively. Even though the pore size of this filler is in the mesoporous range, the increase of hydrogen selectivity can still occur and could be attributed to the penetration of the polymer chains into the MSSs resulting in an enhancement in molecular sieving.

Palladium nanoparticles have also been investigated as another promising material to be used as a constituent in MMMs.[105] This approach is inspired by the highly selective palladium membrane towards hydrogen because of the high hydrogen solubility in palladium. In the study, sub-10 nm palladium nanoparticles were synthesized, and a MMM using PBI as the polymer, with up to 58 wt% particle loading, was successfully fabricated. During the H_2/CO_2 gas separation testing at 225 °C, the H_2 permeability of the MMM is found to be around 94 Barrer, which is an enhancement of around 50% from that of the bare polymeric membrane. This is also

Table 3 Summary of the advantages and disadvantages of various types of fillers used in MMMs for hydrogen separation

Materials	Advantages	Disadvantages/challenges
Zeolites	• High thermal and chemical stability • Well-defined pore structure	• Potential compatibility issues with some polymers, in particular the glassy ones, because of their inorganic nature
	• Good hydrogen molecular sieving capability • Large scale production has been proven	• Limited functionalization potential
Graphite/graphene-based materials	• High mechanical strength • High aspect ratio which could reduce the MMM thickness	• As in zeolites, they may face compatibility issues with some polymers because of their inorganic nature
Metal organic frameworks	• Could offer better compatibility with polymers because of the presence of organic materials • High surface area and porosity • Tunable architecture • Possibility for various functionalizations	• Some MOFs constructed from low valence transition metals (*e.g.* Cu or Zn) are not stable in the presence of moisture or at high pH • Some MOFs have flexible frameworks which could impair their hydrogen molecular sieving capability
Porous organic frameworks	• Could offer better compatibility with polymers because they are completely built from organic materials • The presence of covalent bonding (*e.g.* COFs and PAFs) contributes to building a robust framework • Light weight • Tunable architecture • Possibility for various functionalizations	• Some POFs are still unstable in the presence of moisture or in the case of HOFs, pore collapse might occur because of the absence of strong bonding (*e.g.* coordination and covalent) • Synthesis could be more complex • The pore size of some POFs (*e.g.* COFs) is relatively larger than that of the rest of the fillers and thus could impair their hydrogen molecular sieving capability

accompanied by the enhancement of H_2/CO_2 selectivity from 15 to 30.

Having extensively discussed the fillers used in MMMs for hydrogen separation, it could be concluded that each of them not only offers unique advantages but also faces specific challenges and limitations. Zeolites stand out due to their well-defined pore structures, high stability, and effective molecular sieving capabilities, though their rigidity and inorganic nature create a compatibility challenge with certain polymers. This challenge might also be encountered in the case of MMMs, whose fillers are constructed from other inorganic materials such as graphite and graphene-based materials, although their morphological properties might enable the reduction of membrane thickness. This issue could then be addressed in both MOFs and POFs since they are partially and completely built from organic materials, respectively. In addition, the architecture of both materials is highly tunable, thus enabling the introduction of various functional groups. However, some MOFs face the challenges related to their framework stability in the presence of humidity. Meanwhile, the main challenge in POFs is more related to their synthesis which could be quite complex. A summary of the pros and cons of these fillers is presented in Table 3.

5. Factors affecting the hydrogen separation performance of MMMs

As with other membrane-based processes, the hydrogen separation performance of MMMs can also be heavily influenced by various factors and one important operating parameter is the operating pressure. Since the majority of MMMs comprise polymeric materials, they are also prone to plasticization when operated at high pressure. Plasticization could be understood as a phenomenon where the polymeric chains undergo rearrangement which is caused by the presence of condensable penetrants.[106,107] Therefore, within the context of hydrogen separation from light gases, such a phenomenon might have negative consequences for H_2/CO_2 separation due to the CO_2-induced plasticization phenomenon as exemplified in MMMs loaded with zeolite A where an increase in the operating pressure will also reduce the H_2/CO_2 selectivity.[52] In this case, increasing the operating pressure from 2 to 8 bar reduces the H_2/CO_2 selectivity from around 6 to 1.55. The same negative tendency has also been observed in a GO-loaded PEBAX MMM, where the H_2/CO_2 selectivity of the MMM decreases as the operating pressure increases due to CO_2-induced plasticization.[56]

Therefore, one of the simplest strategies to address this issue is to operate the MMM below its CO_2-induced plasticization pressure. This will avoid the polymeric chain relaxation and thus maintain the MMM performance. Another strategy that is worthy of consideration is to improve the rigidity of the polymer by establishing a strong interaction with the fillers. Both strategies can also be combined so that the CO_2-induced plasticization pressure of the MMM is higher than that of its pristine polymer counterparts. For example, a study involving ZIF-8 in polyimide has shown that the CO_2-induced plasticization pressure of the polymer can be increased from 21 to 30 bar.[38] Similarly, in another investigation using UiO-66-NH_2 and ZIF-8 in the Troger's base polymer, CO_2-induced plasticization also increases from 300 psi to 750 psi.[42] With the increased CO_2-induced plasticization pressure, the MMM could then be operated at higher operating pressure than their pristine polymeric counterparts without the consequence of the deterioration of the hydrogen separation performance. As a result, the positive impacts, as reflected in higher H_2/CO_2 selectivity, could still be observed as exemplified in the case of palladium-loaded-ZIF-8/Matrimid[81] and UiO-66(Hf)–$(OH)_2$.[69] For example, in the case of UiO-66(Hf)–$(OH)_2$/polybenzimidazole, the H_2/CO_2 selectivity can even be increased from around 7.9 to 19.4 as the operating pressure is elevated from 2 to 5 bar, although this must be compromised with a slight reduction of H_2 permeability from around 10.4 to 8.1 Barrer.[69] This might indicate that the absence of CO_2-induced plasticization and the increase in selectivity could be associated with a slower diffusion rate of CO_2 because of the strong adsorption and confined diffusion process within the MOF structure.

Meanwhile, where CO_2 is not involved in the process, an increase in operating pressure can lead to a better hydrogen separation performance since there is no tendency for the plasticization process.[38,50,69,81,104] This has been observed in the case of zeolite A/PDMS; when increasing the differential operating pressure from 0 to 7 bar results in a H_2/CH_4 selectivity improvement from 8.7 to 11.6.[50] This is caused since neither H_2 nor CH_4 plasticizes PDMS. Considering the higher diffusivity of H_2 than CH_4 and the improvement of the molecular sieving contributed by the zeolite in PDMS, the H_2/CH_4 selectivity improvement in the MMM can then be expected. This is because the movement of the polyimide chain can be reduced because of the enhanced molecular interaction with the filler. Similarly, when using HOF-30 as the filler, it has also been observed that the H_2/CH_4 selectivity of the MMM can be increased from around 62 to 72 as the operating pressure is increased from 1 to 3 bar.[104] The selectivity increase is then contributed by the slight enlargement of the pore size of HOF-30 because of its flexible structure, as reflected by the increase of H_2 permeability from around 428 to 580 Barrer. However, such a pore enlargement is not significant enough to also accelerate the permeability process of CH_4, thus increasing selectivity. However, it should also be noted that there can also be a case where an optimum operating condition exists, namely increasing the operating pressure only causes a positive impact to a certain extent. This has been observed in the case of CAU-21-ODB/PIM-1, where the H_2/N_2 selectivity increases from around 7 to 40 by elevating the operating pressure from 0.1 to 0.2 MPa.[62] However, beyond 0.2 MPa, the selectivity continuously decreases and reaches around 22 at 0.4 MPa. This might happen since operating the membrane beyond a certain level might reduce the solubility selectivity while also accelerating the permeation of both gases at the same time.

As in the case of the operating pressure, the operating temperature can also have either positive or negative impacts on the hydrogen separation performance of MMMs. In this

case, the hydrogen separation performance is more impacted by the activation energy of the penetrants. For example, the negative impact of the increasing operating temperature has been observed in zeolite 3A/polysulfone-acrylate.[28] In this case, the diffusivity of light gases increases faster than that of the hydrogen gas resulting in a decrease in the gas selectivity. The same tendency can also be seen in MMMs that are loaded with MOFs.[55,72] In the case of a polyimide membrane loaded with UiO-66-graphite oxide, it has been observed that even though there is a 2-fold increase in H_2 permeability to be around 80 Barrer, the H_2/CH_4 selectivity decreases from around 155 to 80 Barrer.[55] The main cause of this decreasing performance is that the permeability activation energy of light gases is higher than that of hydrogen. Therefore, as the operating temperature is increased, the permeability of the light gases increases more significantly than that of hydrogen, leading to a decrease in selectivity. In a GO/PEBAX MMM, it has also been observed that increasing the operating temperature leads to a slight decrease in both H_2/N_2 and H_2/CH_4 selectivity since hydrogen has a lower permeation activation energy compared to both N_2 and CH_4.[56]

However, it can also be the case that the H_2 permeation activation energy is higher than that of the rest of the light gases. As a result, elevating the operating temperature will lead to an increase in MMM selectivity as was shown in the case of MMMs loaded with various MOFs.[73,80] In addition, such an enhancement might also be caused by the reduction of the solubility selectivity of the MMM at higher temperatures.[80] For example, in a study of ZIF-8/PBI MMM, an increase in temperature led to a reduction in CO_2/H_2 solubility selectivity. Since the diffusivity selectivity of the MMM barely changes, considering the increasing diffusion coefficient of the H_2 at higher temperatures, this leads to an overall increase in the MMM selectivity operated at higher temperatures.

6. Hydrogen separation performance summary of mixed matrix membranes

Having extensively discussed the various types of fillers that can be used in MMMs, the performance summary of these MMMs can then be summarized and the result is presented in Fig. 7. From Fig. 7(A)–(C), it can be seen that there are a significant number of MMMs whose performance can easily surpass the 2008 Robeson upper bound. Moreover, some of them can also get close to the 2015 upper bound that is calculated based on the performance of various microporous polymers for H_2/N_2 and H_2/CH_4 separation.[108] The majority of them come from MMMs that are fabricated using MOFs and POFs as the fillers. Such a trend can be expected considering that MOF-based MMMs constitute the majority of the MMMs studied for hydrogen separation. Moreover, this also indicates that, even though zeolite-based MMMs have been studied before MOF-based MMMs, they do not perform as well as MOF-based MMMs in elevating the hydrogen separation performance of polymeric membranes. There might be various causes for this, but the polymer-zeolite compatibility issue might play a significant role since, unlike MOFs or POFs, zeolites do not have organic components within their structure and thus might pose a challenge in establishing a good interaction with polymers. If this happens, even though zeolites with correct pore apertures

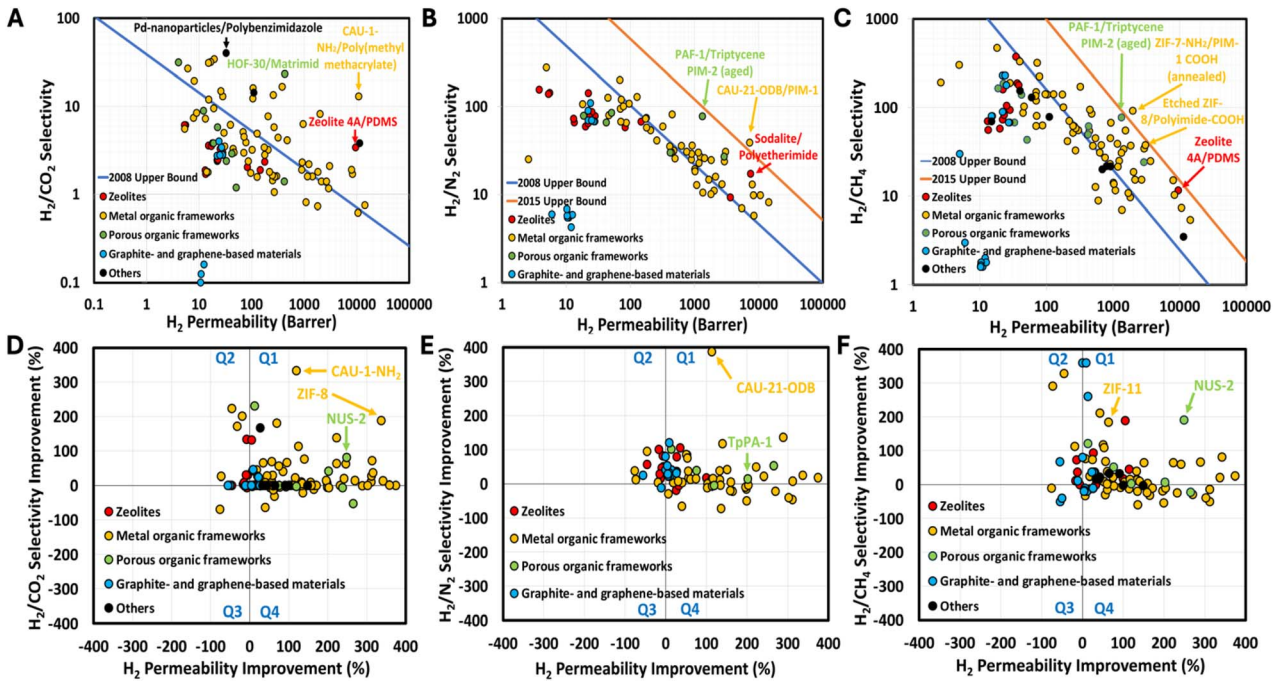

Fig. 7 The hydrogen separation performance summary of MMMs: the permeability-selectivity trade-off plotted against the upper bounds for H_2/CO_2 (A), H_2/N_2 (B) and H_2/CH_4 (C) separation processes and the permeability-selectivity improvement relative to their corresponding bare polymeric membranes for H_2/CO_2 (D), H_2/N_2 (E) and H_2/CH_4 (F) separation processes.

are used as fillers, imperfections at the zeolite–polymer interface might mask the molecular sieving impact from the zeolites.

In addition to the performance analysis against the upper bound, the MMM hydrogen separation performance can also be further evaluated based on the improvement of both the hydrogen permeability and selectivity. The result of this evaluation is presented in Fig. 7(D)–(F). It can be seen from the results that the majority of MMMs are well-placed within the Q1 of the diagram, thus indicating the positive impact of fillers in simultaneously enhancing both the hydrogen permeability and selectivity of bare polymeric membranes. Some of the fillers from the MOF and POF families have also exhibited a more pronounced performance improvement than the rest such as in the cases of CAU-1-NH_2, CAU-21-ODB, ZIF-8 and ZIF-11 and COF NUS-2. In the cases of CAU-1-NH_2 and CAU-21-ODB, it can also be observed that the selectivity improvement can reach around 300–400%. Such an improvement might be related to the correct pore aperture of both MOFs which falls around 0.3–0.4 nm and enables them to improve the molecular sieving properties of the membranes. In addition, it is also possible that the absence of framework flexibility, as observed in some ZIF MOFs, might contribute to a better hydrogen separation improvement observed in CAU-based MMMs rather than ZIF-based MMMs. Meanwhile, in the case of MMMs loaded with POFs such as NUS-2 and TpPA-1, it seems that the hydrogen permeability improvement is slightly more pronounced than that of CAU-based MMMs. This might be associated with the larger pore aperture of POFs in comparison to MOFs, thus enabling faster diffusion of the hydrogen gas in POF-based MMMs. It is also worth mentioning that, even though the pore aperture of POFs is relatively larger than that of MOFs, the improvement in the hydrogen selectivity can still be expected. However, such an improvement is more attributed to the engineering of the MMM gas affinity rather than molecular sieving. For example, as has been previously discussed in the case of NUS-2 MMM,[100] the H_2/CO_2 selectivity improvement of the MMM happens because NUS-2 interacts strongly with CO_2 and thus hinders its permeation while it provides more additional pathways for the permeation of H_2. As a result, the H_2/CO_2 selectivity of the MMM is higher than that of the bare polymeric membranes.

The hydrogen separation performance of MMMs can also be further scrutinized by looking closely into two important physical properties of the fillers, namely the surface area and the pore size. However, before further discussing the impact of such physical properties on the hydrogen separation performance of MMMs, it should be noted that there are at least two limitations associated with this analysis. First, this analysis can only be performed by evaluating the data from the studies where both physical properties of the fillers are fully characterized -which is usually carried out through nitrogen or argon physisorption- and reported. This then leads to the second limitation associated with the type of filler that can be included in this evaluation. Given that both the surface area and pore size characterization are typically conducted on various porous materials (*e.g.* zeolites, MOFs and POFs), this also means that this evaluation is mostly based on MMMs constructed using

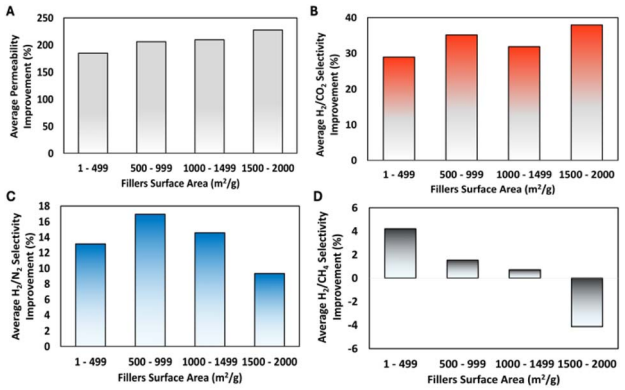

Fig. 8 The impact of filler surface area on the improvement of MMM's hydrogen permeability (A) and hydrogen selectivity against CO_2 (B), N_2 (C) and CH_4 (D).

porous materials as fillers. Nevertheless, conducting this analysis remains crucial. This is because, as previously discussed, these materials constitute the majority of the fillers used in MMMs for hydrogen separation and the resulting membranes also demonstrate promising hydrogen separation performance. Therefore, this analysis is essential for gaining a deeper understanding of how the physical properties of these fillers influence the hydrogen separation performance of MMMs. The results for the effect of the surface area and the pore size of the fillers on the hydrogen separation performance of MMMs are then presented in Fig. 8 and 9, respectively.

First, from Fig. 8(A), it can be observed that there is a positive correlation between the filler surface area and the increase of the MMM hydrogen permeability. This means that MMMs that are fabricated with fillers with higher surface areas experience a higher increase in hydrogen permeability. Such a positive correlation is expected because fillers with higher surface area could provide more free volume in the MMM which might contribute to enhancing gas diffusional pathways, resulting in higher hydrogen permeability. However, it can also be seen from the rest of Fig. 8 that both inconclusive and decreasing trends of the hydrogen selectivity of the MMM can happen as

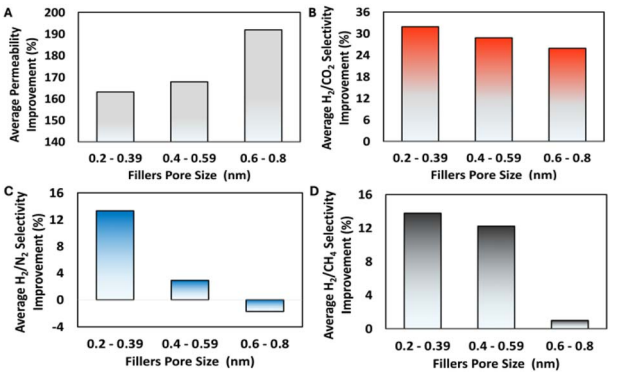

Fig. 9 The impact of filler pore size on the improvement of MMM's hydrogen permeability (A) and hydrogen selectivity against CO_2 (B), N_2 (C) and CH_4 (D).

the surface area of the fillers increases, as exemplified in Fig. 8(B) and (D), respectively. This might be caused since porous materials with large surface area could have either small or large pore size or a combination of both. For example, in the case of ZIF-8, the combination of a large surface area and small pore size might lead to the improvement in the hydrogen selectivity in the MMM.[78] In contrast, in the case of MIL-101(Cr), where there is a combination of large surface area and large pore size, the use of such fillers might lead to a decrease in hydrogen selectivity because of the deterioration of the molecular sieving capability of the MMM.[63] From this analysis, it can be safely inferred that the surface area of the fillers positively influences the hydrogen permeability of the MMM. Therefore, fillers with a high surface area are required to obtain MMMs with high hydrogen permeability. However, a direct conclusion regarding the impact of the filler surface area on the hydrogen selectivity cannot be drawn since it must also consider the pore aperture of the filler.

In addition to the filler surface area, the filler pore size is also another important physical property that might affect the hydrogen separation performance of MMMs. The analysis result showing the correlation between the filler pore size and the MMM hydrogen permeability and selectivity is then given in Fig. 9. As can be seen in Fig. 9(A), there is also a positive correlation between the filler pore size and the increase in the hydrogen permeability of the MMM. As in the case of filler surface area, such a positive correlation can be explained by the increase in the gas diffusion rate as the filler pore size gets higher. However, differing from this trend and the inconclusive trend shown in Fig. 8(B)–(D), it can be seen from Fig. 9(B)–(D) that there is a negative correlation between the filler pore size and the increase in hydrogen selectivity of the MMM. This means that a filler with a smaller pore size is more effective in increasing the hydrogen selectivity of MMMs which could be associated with the ability of fillers to improve the molecular sieving properties of MMMs. This analysis then corroborates the previous discussion where a MMM that is loaded with a POF typically exhibits higher hydrogen permeability improvement than an MOF-based MMM, considering the pore size of the former is generally highre than that of the latter. Moreover, this also complements the previous analysis regarding the impact of the filler surface area on the hydrogen selectivity of the MMM since a clearer trend can be observed from this analysis, namely, smaller pore size leads to the improvement of the MMM hydrogen selectivity, showing that the hydrogen selectivity of the MMM is much more affected by the filler pore size than the filler surface area.

All these analyses might then suggest that MMMs that are loaded with fillers having the correct combination of high surface area and correct pore size should have the capability to simultaneously increase both the hydrogen permeability and selectivity and therefore warrant further investigations. In this case, the use of MOFs and POFs as porous fillers for MMMs could be more promising and offer more advantages than other porous materials. In addition to their tailorable architecture which enables them to be designed with the intended physical properties, this is also because both materials are constructed with organic compounds -or at least partially in the case of MOFs- thus also offering numerous possibilities for functionalization which could further enhance the filler-polymer interaction and also improve the hydrogen separation performance of MMMs.

7. Challenges and outlook of MMMs for hydrogen separation

Despite the promising hydrogen separation performance exhibited by most MMMs using various promising fillers such as MOFs and POFs, some challenges remain that must be addressed in the future to further prove the readiness of such MMMs to be deployed in real situations. The first challenge could be related to the fabrication process of MMMs. In this case, one of the main issues is regarding the poor interfacial adhesion which can result in the formation of non-selective voids or rigidified polymer layers around the filler particles. This issue becomes more pronounced as the particle loading increases. Such conditions can negatively affect the hydrogen separation performance of MMMs. Functionalization of the filler has been employed to diminish this issue which showed promising results. As an example, in a UiO-66-$(OH)_2$/6FDA-DAM : DABA(3 : 2) MMM, the effect of filler loading has been explored by using hydroxyl functionalized UiO-66 nanoparticles. Gas separation results showed that on increasing the MOF loading from 40 to 50 wt%, not only did the H_2 permeability not decrease, but it also nearly doubled from 497 to 907 Barrer. Also, the H_2/N_2 and H_2/CH_4 selectivities increased from 26 and 37 to 29 and 45, respectively, as the MOF loading was increased.[68] Although filler functionalization proved to be a good method to enhance interfacial adhesion, the development of universal and scalable strategies to ensure strong filler-polymer interaction remains an open challenge since not all the fillers can functionalize in the same way and with the same functional group.

Another key challenge is to fabricate MMMs in the form of a thin film and a hollow fiber geometry since this research direction has not been fully explored. There are at least two advantages in fabricating MMMs in these forms. First, as the MMM thickness is reduced, the membrane resistance for gas permeation also decreases, thus increasing its gas permeance. Second, fabricating MMMs in the hollow fiber geometry also provides an advantage since hollow fiber geometry offers a high surface area to volume ratio and thus is more attractive from a practical point of view.[109] In this context, there are already few studies showing a promising performance of hollow fiber MMMs for hydrogen separation. For instance, a zeolite-based MMM has been fabricated by combining a carbon-impregnated zeolite and P-84 polymer. The H_2 permeability of the MMM is found to be around 27 Barrer and its H_2 selectivity against both N_2 and CH_4 falls around 58.[53] As illustrated in Fig. 10, hollow fiber MMMs have also been fabricated by combining ZIF-8 and polybenzimidazole for H_2/CO_2 separation which can be operated up to 30 bar and 150 °C without showing any performance deterioration.[76,80,82] In this case, the H_2 permeance and H_2/CO_2 selectivity of the MMM are reported to be in the range of 22–200 GPU and 13–32, respectively. Interestingly, it has also been observed that operating one of these MMMs at

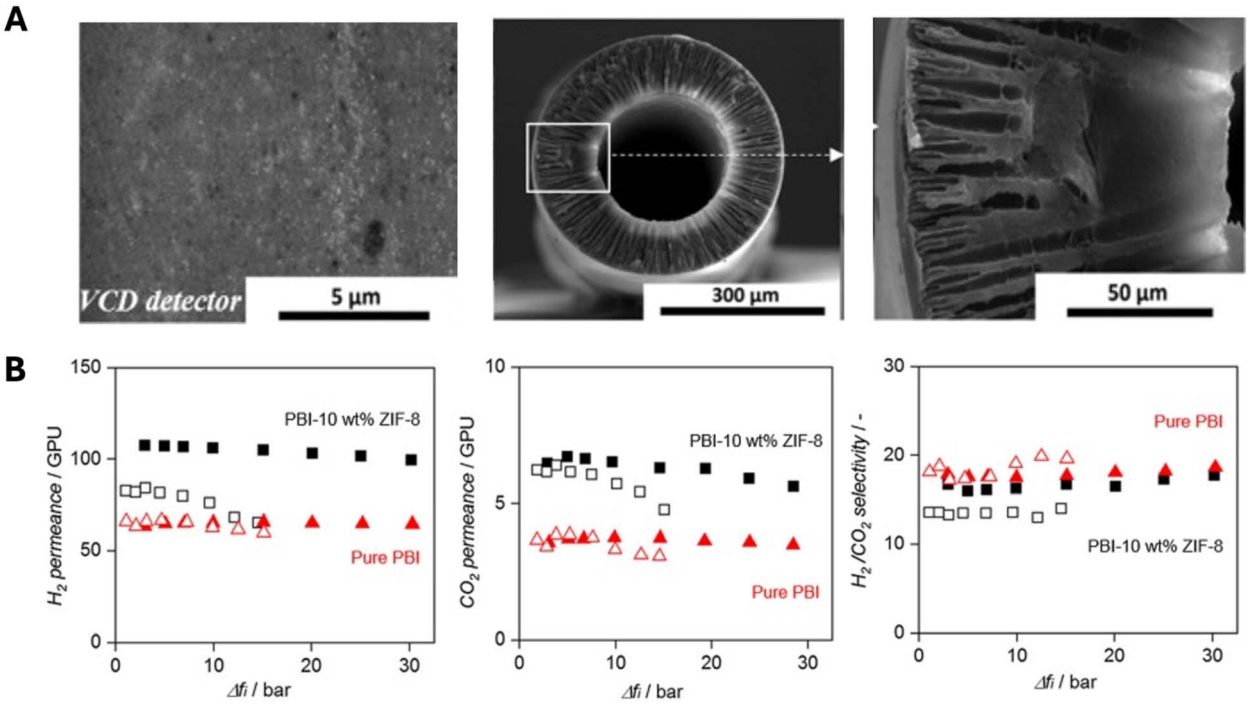

Fig. 10 SEM micrographs of a 10 wt% ZIF-8/PBI MMM (A) and its corresponding H_2/CO_2 separation performance (B). The figure is produced with permission.[76] Copyright 2019 The authors and Elsevier.

a higher temperature might be beneficial since it can increase the H_2 permeance without any significant reduction in the H_2/CO_2 selectivity.[76] The capability of these MMMs to withstand high temperature operation is indeed very attractive from the practical point of view, particularly if they are going to be deployed for pre-combustion CO_2 capture since this process requires relatively high operating temperature.[110]

In addition to the challenge related to MMM fabrication, another challenge can also be found regarding the stability of the hydrogen separation performance of MMMs, particularly in relation to the physical aging phenomenon. Physical aging is a condition where the polymeric chains in a polymeric membrane undergo a molecular rearrangement over time. This phenomenon is more pronounced to be encountered in high free-volume polymers such as polymers of intrinsic microporosity and the rate of physical aging is more accelerated in a thin film rather than a thick-film membrane. Such a molecular rearrangement usually leads to the reduction of the membrane's free volume. Consequently, a reduction in hydrogen permeability and an increase in hydrogen selectivity are usually observed. For example, in one study using PAF-1 as a filler, it was observed that after two months, even though the H_2/N_2 and H_2/CH_4 selectivity of the 5 wt% PAF-1 MMM significantly increased from 27 to 78 and 24.2 to 77.8, respectively, the H_2 permeability of the membrane decreased more than twice from 2907 to 1335 Barrer.[94] Along with the issue of CO_2-induced plasticization—which, as previously discussed, occurs when MMMs are operated at high pressure—these challenges highlight the need to develop MMMs with stable hydrogen separation performance. Considering the similarities between physical aging and CO_2-induced plasticization issues, namely related to the rearrangement of the polymeric chains, it might be possible to simultaneously address both issues by enhancing the rigidity of the polymeric chains which could be accomplished by establishing a strong interaction between the fillers and the polymer chains. As has been studied, such an approach is effective in increasing the resistance of MMMs against CO_2-induced plasticization and thus might as well be effective in tackling the physical aging issue encountered in MMMs.[63,111]

Furthermore, the stability of the hydrogen separation performance of MMMs must also be comprehensively evaluated under various testing conditions, particularly under the conditions where they are going to be applied. For example, in the case where MMMs are targeted to be used in the pre-combustion process to separate H_2 from CO_2, testing them at high temperature would be very crucial to observe whether performance deterioration exists under elevated temperature conditions. Moreover, it is also worth investigating the impact of the presence of other components in the feed mixture on the hydrogen separation performance of MMMs under such conditions.

Once the above challenges have been successfully addressed, as a final note, it also becomes important to address the challenge of scaling up the fabrication process of the most promising MMMs. In this case, a comprehensive techno-economic analysis may be necessary, as some fillers—particularly those from the MOF and POF classes—might require specific chemicals that are not yet produced on a large scale. Therefore, it becomes crucial to find a balance between the economic aspect of producing MMMs and their hydrogen separation performance.

8. Conclusions

With the growing concern of climate change and the continuously increasing global temperature, the transition from a fossil fuel-based economy towards a green economy needs to be significantly accelerated. Within this context, the utilization of hydrogen as one of the cleanest energy carriers has to be expedited and thus requires advancement not only in terms of hydrogen production but also its separation from other gases. Membrane technology could then be used as one of the main tools to realize this objective. During the last few years, a significant advancement has been made in the field of MMMs for hydrogen separation. Various materials such as zeolites, MOFs, POFs and graphite- and graphene-based materials have been studied to improve the hydrogen separation performance of bare polymeric membranes. Among these materials, MOFs and POFs will show great promise in the future since there is a possibility to synthesize both materials with high surface area and correct pore aperture, which are two important physical properties of fillers that could significantly influence the hydrogen separation performance of MMMs. Despite this, some challenges that might significantly impact the stability of the MMM performance such as physical aging and CO_2-induced plasticization have yet to be addressed in the future. In addition, it is also important to systematically study MMM fabrication in the form of thin films and hollow fiber geometry. By directing research in this direction, it could be expected that the implementation of MMMs for hydrogen separation could also be fully realized.

Data availability

The data used to plot the graphs in this article are available in the ESI.†

Author contributions

R. S.: conceptualization, methodology, software, validation, formal analysis, investigation, data curation, writing – original draft, writing – reviewing & editing, visualization. B. P. L.: conceptualization, writing – reviewing & editing, supervision, project administration, funding acquisition. N. P.: conceptualization, methodology, software, validation, formal analysis, investigation, data curation, writing – original draft, writing – reviewing & editing, visualization, supervision.

Conflicts of interest

There are no conflicts to declare.

Acknowledgements

R. S acknowledges the funding from the Luxembourg National Research Fund (Fonds National de la Recherche, FNR). All the authors also acknowledge the funding from the Paul Wurth Chair, University of Luxembourg.

Notes and references

1 Y. Li, G. He, S. Wang, S. Yu, F. Pan, H. Wu and Z. Jiang, *J. Mater. Chem. A*, 2013, **1**, 10058–10077.
2 H. B. T. Jeazet, C. Staudt and C. Janiak, *Dalton Trans.*, 2012, **41**, 14003–14027.
3 L. M. Robeson, *J. Membr. Sci.*, 2008, **320**, 390–400.
4 N. Prasetya, I. G. Wenten and B. P. Ladewig, *Energy Environ. Mater.*, 2024, e12843.
5 J. C. Maxwell, *A Treatise on Electricity and Magnetism*, Oxford University Press, London, 1873.
6 H. Vinh-Thang and S. Kaliaguine, *Chem. Rev.*, 2013, **113**, 4980–5028.
7 D. A. G. Bruggeman, *Ann. Phys.*, 1935, **416**, 636–664.
8 T. B. Lewis and L. E. Nielsen, *J. Appl. Polym. Sci.*, 1970, **14**, 1449–1471.
9 R. Pal, *J. Reinf. Plast. Compos.*, 2007, **26**, 643–651.
10 Y. Li, T. Chung, C. Cao and S. Kulprathipanja, *J. Membr. Sci.*, 2005, **260**, 45–55.
11 Y. Li, H.-M. Guan, T.-S. Chung and S. Kulprathipanja, *J. Membr. Sci.*, 2006, **275**, 17–28.
12 S. N. Wijenayake, N. P. Panapitiya, S. H. Versteeg, C. N. Nguyen, S. Goel, K. J. Balkus, I. H. Musselman and J. P. Ferraris, *Ind. Eng. Chem. Res.*, 2013, **52**, 6991–7001.
13 X. Wang, L. Wu, N. Li and Y. Fan, *J. Membr. Sci.*, 2021, **636**, 119582.
14 D. Zhao, J. Ren, Y. Qiu, H. Li, K. Hua, X. Li and M. Deng, *J. Appl. Polym. Sci.*, 2015, **132**, 42624.
15 Q. Zhang, S. Luo, J. R. Weidman and R. Guo, *Polymer*, 2017, **131**, 209–216.
16 J. S. Kim, S. J. Moon, H. H. Wang, S. Kim and Y. M. Lee, *J. Membr. Sci.*, 2019, **582**, 381–390.
17 N. Ercan, C. Kocyigit, A. Durmus and A. Kasgoz, *J. Nat. Gas Sci. Eng.*, 2021, **95**, 104155.
18 T. Yang, Y. Xiao and T.-S. Chung, *Energy Environ. Sci.*, 2011, **4**, 4171.
19 L. Diestel, N. Wang, A. Schulz, F. Steinbach and J. Caro, *Ind. Eng. Chem. Res.*, 2015, **54**, 1103–1112.
20 Y. Fan, H. Yu, S. Xu, Q. Shen, H. Ye and N. Li, *J. Membr. Sci.*, 2020, **597**, 117775.
21 K. Zhang, X. Tian, Z. Xu, H. Huan, R. Zhang, X. Feng, Q. Wang, Y. Tang, C. Liu and S. Wang, *Adv. Funct. Mater.*, 2025, **35**, 2417186.
22 C. I. Chaidou, G. Pantoleontos, D. E. Koutsonikolas, S. P. Kaldis and G. P. Sakellaropoulos, *Sep. Sci. Technol.*, 2012, **47**, 950–962.
23 G. Yang, H. Guo, Z. Kang, L. Zhao, S. Feng, F. Jiao and S. Mintova, *ChemSusChem*, 2019, **12**, 4529–4537.
24 L. Zhu, D. Yin, Y. Qin, S. Konda, S. Zhang, A. Zhu, S. Liu, T. Xu, M. T. Swihart and H. Lin, *Adv. Funct. Mater.*, 2019, **29**, 1904357.
25 Z. Kang, Y. Peng, Z. Hu, Y. Qian, C. Chi, L. Y. Yeo, L. Tee and D. Zhao, *J. Mater. Chem. A*, 2015, **3**, 20801–20810.
26 H. Yin, A. Alkaş, Y. Zhang, Y. Zhang and S. G. Telfer, *J. Membr. Sci.*, 2020, **609**, 118245.

27 A. Perea-Cachero, J. Sánchez-Laínez, Á. Berenguer-Murcia, D. Cazorla-Amorós, C. Téllez and J. Coronas, *J. Membr. Sci.*, 2017, **544**, 88–97.
28 A. L. Khan, A. Cano-Odena, B. Gutiérrez, C. Minguillón and I. F. Vankelecom, *J. Membr. Sci.*, 2010, **350**, 340–346.
29 C. Chaidou, G. Pantoleontos, D. Koutsonikolas, S. Kaldis and G. Sakellaropoulos, *Sep. Sci. Technol.*, 2012, **47**, 950–962.
30 C. Ma and J. J. Urban, *Adv. Funct. Mater.*, 2019, **29**, 1903243.
31 M. Peydayesh, T. Mohammadi and O. Bakhtiari, *Energy*, 2017, **141**, 2100–2107.
32 M. J. C. Ordonez, K. J. Balkus Jr, J. P. Ferraris and I. H. Musselman, *J. Membr. Sci.*, 2010, **361**, 28–37.
33 H. Junoh, J. Jaafar, H. Mohamed and K. P. Jern, *Mater. Today: Proc.*, 2024, **96**, 84–89.
34 N. Ercan, C. Kocyigit, A. Durmus and A. Kasgoz, *J. Nat. Gas Sci. Eng.*, 2021, **95**, 104155.
35 C. Rubio, B. Zornoza, P. Gorgojo, C. Tellez and J. Coronas, *Curr. Org. Chem.*, 2014, **18**, 2351–2363.
36 Y. Fan, H. Yu, S. Xu, Q. Shen, H. Ye and N. Li, *J. Membr. Sci.*, 2020, **597**, 117775.
37 B. Zornoza, C. Téllez, J. Coronas, O. Esekhile and W. J. Koros, *AIChE J.*, 2015, **61**, 4481–4490.
38 Y. Shi, S. Wu, Z. Wang, X. Bi, M. Huang, Y. Zhang and J. Jin, *Sep. Purif. Technol.*, 2021, **277**, 119449.
39 L. Diestel, N. Wang, A. Schulz, F. Steinbach and J. Caro, *Ind. Eng. Chem. Res.*, 2015, **54**, 1103–1112.
40 X. Wang, L. Wu, N. Li and Y. Fan, *J. Membr. Sci.*, 2021, **636**, 119582.
41 X. Jiang, S. He, G. Han, J. Long, S. Li, C. H. Lau, S. Zhang and L. Shao, *ACS Appl. Mater. Interfaces*, 2021, **13**, 11296–11305.
42 Z. Wang, D. Wang, S. Zhang, L. Hu and J. Jin, *Adv. Mater.*, 2016, **28**, 3399–3405.
43 J. Yu, J. Kim, N. Lee, K. Eum and Y.-H. Ahn, *J. Environ. Chem. Eng.*, 2024, 113167.
44 S. Park, K. Y. Cho and H.-K. Jeong, *J. Mater. Chem. A*, 2020, **8**, 11210–11217.
45 Y. Liu, W. Xie, S. Liang, X. Li, Y. Fan and S. Luo, *J. Membr. Sci.*, 2022, **646**, 120240.
46 Q. Zhao, Y. Sun, J. Zhang, F. Fan, T. Li, G. He and C. Ma, *J. Membr. Sci.*, 2024, **693**, 122326.
47 Y. Jia, P. Liu, Y. Liu, D. Zhang, Y. Ning, C. Xu and Y. Zhang, *Fuel*, 2023, **339**, 126938.
48 C. Eden and M. Daramola, *Mater. Today: Proc.*, 2021, **38**, 522–527.
49 G. Yang, H. Guo, Z. Kang, L. Zhao, S. Feng, F. Jiao and S. Mintova, *ChemSusChem*, 2019, **12**, 4529–4537.
50 M. Rezakazemi, K. Shahidi and T. Mohammadi, *Int. J. Hydrogen Energy*, 2012, **37**, 14576–14589.
51 M. Rezakazemi, K. Shahidi and T. Mohammadi, *Int. J. Hydrogen Energy*, 2012, **37**, 17275–17284.
52 J. Ahmad and M.-B. Hägg, *J. Membr. Sci.*, 2013, **427**, 73–84.
53 T. Gunawan, N. Widiastuti, A. R. Widyanto, H. Fansuri, S. Akhlus, W. N. W. Salleh, A. F. Ismail, N. Sazali, R. Lin, J. Motuzas and S. Smart, *Chem. Eng. Res. Des.*, 2024, **204**, 556–571.
54 B. M. Yoo, J. E. Shin, H. D. Lee and H. B. Park, *Curr. Opin. Chem. Eng.*, 2017, **16**, 39–47.
55 S. Castarlenas, C. Téllez and J. Coronas, *J. Membr. Sci.*, 2017, **526**, 205–211.
56 D. Zhao, J. Ren, Y. Qiu, H. Li, K. Hua, X. Li and M. Deng, *J. Appl. Polym. Sci.*, 2015, **132**, app.42624.
57 G. Huang, A. P. Isfahani, A. Muchtar, K. Sakurai, B. B. Shrestha, D. Qin, D. Yamaguchi, E. Sivaniah and B. Ghalei, *J. Membr. Sci.*, 2018, **565**, 370–379.
58 X. Y. Chen, T. B. Nguyen, A. Romero, A. Paton, M. Sanchez, J. Valverde, S. Kaliaguine and D. Rodrigue, *J. Membr. Sci. Res.*, 2020, **6**, 58–69.
59 R. Rohani, H. M. Kalkhoran and Y. T. Chung, *J. Teknol. Lab.*, 2019, **81**(3), DOI: **10.11113/jt.v81.12895**.
60 L. Cao, K. Tao, A. Huang, C. Kong and L. Chen, *Chem. Commun.*, 2013, **49**, 8513–8515.
61 Y. Zhao, D. Zhao, C. Kong, F. Zhou, T. Jiang and L. Chen, *Sep. Purif. Technol.*, 2019, **220**, 197–205.
62 C. Zhang, B. Liu, G. Wang, G. Yu, X. Zou and G. Zhu, *Chem. Commun.*, 2019, **55**, 7101–7104.
63 J. Lee, S. Jeon, E. J. An, H. G. Kim, J. H. Jo, N. Han, S. Park and W. S. Chi, *Sep. Purif. Technol.*, 2025, **356**, 129854.
64 Y. Zhou, Z. Hu, M. Yu, L. Zhang and J. Yao, *Cellulose*, 2023, **30**, 201–209.
65 E. Aliyev, J. Warfsmann, B. Tokay, S. Shishatskiy, Y.-J. Lee, J. Lillepaerg, N. R. Champness and V. Filiz, *ACS Sustain. Chem. Eng.*, 2020, **9**, 684–694.
66 M. Arjmandi, M. Pakizeh, M. Saghi and A. Arjmandi, *Petrol. Chem.*, 2018, **58**, 317–329.
67 X. Wang, W. Huang, X. Li, X. Li, X. Chai, Y. Zhou, J. Zhong and R. Zhou, *J. Membr. Sci.*, 2025, **713**, 123351.
68 C. Ma and J. J. Urban, *ChemSusChem*, 2019, **12**, 4405–4411.
69 Z. Hu, Z. Kang, Y. Qian, Y. Peng, X. Wang, C. Chi and D. Zhao, *Ind. Eng. Chem. Res.*, 2016, **55**, 7933–7940.
70 S. Kim, E. Shamsaei, X. Lin, Y. Hu, G. P. Simon, J. G. Seong, J. S. Kim, W. H. Lee, Y. M. Lee and H. Wang, *J. Membr. Sci.*, 2018, **549**, 260–266.
71 J. Deng, Z. Dai and L. Deng, *J. Membr. Sci.*, 2020, **610**, 118262.
72 T. Yang, Y. Xiao and T.-S. Chung, *Energy Environ. Sci.*, 2011, **4**, 4171–4180.
73 S. Park, H. An, J. Seong, S. Kim, J. Choi and J. S. Lee, *Microporous Mesoporous Mater.*, 2024, **379**, 113267.
74 B. A. Al-Maythalony, A. M. Alloush, M. Faizan, H. Dafallah, M. A. Elgzoly, A. A. Seliman, A. Al-Ahmed, Z. H. Yamani, M. A. Habib and K. E. Cordova, *ACS Appl. Mater. Interfaces*, 2017, **9**, 33401–33407.
75 S. N. Wijenayake, N. P. Panapitiya, S. H. Versteeg, C. N. Nguyen, S. Goel, K. J. Balkus Jr, I. H. Musselman and J. P. Ferraris, *Ind. Eng. Chem. Res.*, 2013, **52**, 6991–7001.
76 M. Etxeberria-Benavides, T. Johnson, S. Cao, B. Zornoza, J. Coronas, J. Sanchez-Lainez, A. Sabetghadam, X. Liu, E. Andres-Garcia and F. Kapteijn, *Sep. Purif. Technol.*, 2020, **237**, 116347.
77 X. Mei, S. Yang, P. Lu, Y. Zhang and J. Zhang, *Front. Chem.*, 2020, **8**, 528.

78 A. F. Bushell, M. P. Attfield, C. R. Mason, P. M. Budd, Y. Yampolskii, L. Starannikova, A. Rebrov, F. Bazzarelli, P. Bernardo and J. C. Jansen, *J. Membr. Sci.*, 2013, **427**, 48–62.
79 J. S. Kim, S. J. Moon, H. H. Wang, S. Kim and Y. M. Lee, *J. Membr. Sci.*, 2019, **582**, 381–390.
80 T. Yang, G. M. Shi and T. Chung, *Adv. Energy Mater.*, 2012, **2**, 1358–1367.
81 A. Mirzaei, A. H. Navarchian and S. Tangestaninejad, *Iran. Polym. J.*, 2020, **29**, 479–491.
82 A. Perea-Cachero, M. Etxeberría-Benavides, O. David, A. Deacon, T. Johnson, M. Malankowska, C. Téllez and J. Coronas, *R. Soc. Open Sci.*, 2021, **8**, 210660.
83 Z. Li, Y. Guo, J. Yu, X. Ruan, X. Jiang, Y. Dai, T. Li, X. Li, W. Zheng and G. He, *J. Membr. Sci.*, 2024, **707**, 123000.
84 G. Moral, A. Ortiz, D. Gorri and I. Ortiz, *Sep. Purif. Technol.*, 2025, **362**, 131890.
85 M. S. Boroglu and A. B. Yumru, *Sep. Purif. Technol.*, 2017, **173**, 269–279.
86 A. B. Yumru, M. Safak Boroglu and I. Boz, *Greenh. Gases: Sci. Technol.*, 2018, **8**, 529–541.
87 J. Sánchez-Laínez, B. Zornoza, A. F. Orsi, M. M. Łozińska, D. M. Dawson, S. E. Ashbrook, S. M. Francis, P. A. Wright, V. Benoit and P. L. Llewellyn, *Chem.–Eur. J.*, 2018, **24**, 11211–11219.
88 M. Safak Boroglu, I. Boz and B. Kaya, *J. Polym. Eng.*, 2021, **41**, 259–270.
89 K. Zhang, X. Tian, Z. Xu, H. Huan, R. Zhang, X. Feng, Q. Wang, Y. Tang, C. Liu and S. Wang, *Adv. Funct. Mater.*, 2025, **35**, 2417186.
90 Q. Zhang, S. Luo, J. R. Weidman and R. Guo, *Polymer*, 2017, **131**, 209–216.
91 T. Wu, N. Prasetya and K. Li, *J. Membr. Sci.*, 2020, **615**, 118493.
92 S. Zhang, Q. Yang, C. Wang, X. Luo, J. Kim, Z. Wang and Y. Yamauchi, *Advanced Science*, 2018, **5**, 1801116.
93 Y. Tian and G. Zhu, *Chem. Rev.*, 2020, **120**, 8934–8986.
94 R. Hou, B. S. Ghanem, S. J. Smith, C. M. Doherty, C. Setter, H. Wang, I. Pinnau and M. R. Hill, *J. Mater. Chem. A*, 2020, **8**, 14713–14720.
95 A. P. Côté, A. I. Benin, N. W. Ockwig, M. O'Keeffe, A. J. Matzger and O. M. Yaghi, *Science*, 2005, **310**, 1166–1170.
96 S. Yuan, X. Li, J. Zhu, G. Zhang, P. Van Puyvelde and B. Van Der Bruggen, *Chem. Soc. Rev.*, 2019, **48**, 2665–2681.
97 S.-Y. Ding and W. Wang, *Chem. Soc. Rev.*, 2013, **42**, 548–568.
98 G. Li, J. Kujawa, K. Knozowska, A. Kareiva, E. Favre, C. Castel and W. Kujawski, *Carbon Capture Sci. Technol.*, 2024, **13**, 100267.
99 B. P. Biswal, H. D. Chaudhari, R. Banerjee and U. K. Kharul, *Chem.–Eur. J.*, 2016, **22**, 4695–4699.
100 Z. Kang, Y. Peng, Y. Qian, D. Yuan, M. A. Addicoat, T. Heine, Z. Hu, L. Tee, Z. Guo and D. Zhao, *Chem. Mater.*, 2016, **28**, 1277–1285.
101 R.-B. Lin and B. Chen, *Chem*, 2022, **8**, 2114–2135.
102 R.-B. Lin, Y. He, P. Li, H. Wang, W. Zhou and B. Chen, *Chem. Soc. Rev.*, 2019, **48**, 1362–1389.
103 Y. Hou, X.-S. Huang, S.-H. Gong, C. Liu, Y. Liu and T.-F. Liu, *Nano Res.*, 2024, 1–25.
104 W. Li, Y. Li, J. Caro and A. Huang, *J. Membr. Sci.*, 2022, **643**, 120021.
105 L. Zhu, D. Yin, Y. Qin, S. Konda, S. Zhang, A. Zhu, S. Liu, T. Xu, M. T. Swihart and H. Lin, *Adv. Funct. Mater.*, 2019, **29**, 1904357.
106 K. M. Rodriguez, S. Lin, A. X. Wu, K. R. Storme, T. Joo, A. F. Grosz, N. Roy, D. Syar, F. M. Benedetti and Z. P. Smith, *Chem. Soc. Rev.*, 2024, **53**, 2435–2529.
107 Y. S. Chang, P. Kumari, C. J. Munro, G. Szekely, L. F. Vega, S. Nunes and L. F. Dumée, *J. Membr. Sci.*, 2023, **666**, 121125.
108 R. Swaidan, B. Ghanem and I. Pinnau, *ACS Macro Lett.*, 2015, **4**, 947–951.
109 H. S. Lau and W. F. Yong, *J. Mater. Chem. A*, 2021, **9**, 26454–26497.
110 N. Prasetya, N. F. Himma, P. D. Sutrisna, I. G. Wenten and B. P. Ladewig, *Chem. Eng. J.*, 2020, **391**, 123575.
111 Y. Ying, Y. Cheng, S. B. Peh, G. Liu, B. B. Shah, L. Zhai and D. Zhao, *J. Membr. Sci.*, 2019, **582**, 103–110.